

3D FEM Analyses of the Buckling Delamination of a Rectangular Sandwich Plate Containing Interface Rectangular Cracks and Made from Elastic and Viscoelastic Materials

Surkay D. Akbarov^{1,2}, Nazmiye Yahnioglu³ and Ayfer Tekin⁴

Abstract: A three-dimensional buckling delamination problem for the sandwich rectangular plate made from elastic and viscoelastic material is studied. It is supposed that the plate contains interface rectangular cracks (Case 1) and interface rectangular edge-cracks (Case 2) and edge-surfaces of these cracks have initial infinitesimal imperfections. The evolution of these initial imperfections with an external compressive loading acting along the cracks (for a case where the materials of layers of the plate are elastic) or with duration of time (for a case where the materials of layers of the plate are viscoelastic) is investigated within the framework of the piecewise homogeneous body model with the use of three-dimensional geometrically nonlinear field equations of the theory of the viscoelastic bodies. For the determination of the values of the critical force or critical time as well as the buckling delamination mode, the initial imperfection criterion is used. The corresponding boundary-value problems are solved by employing boundary form perturbation techniques, Laplace transform and FEM. The influence of the materials or geometrical parameters of the plate on the critical values is discussed. In particular, it is established that for the considered change range of the problem parameters the buckling form depends not only on the infinitesimal initial imperfection mode of the crack edges, but also on the parameters which characterize the geometry and location of these cracks.

¹ Corresponding author. Yildiz Technical University, Faculty of Mechanical Engineering, Department of Mechanical Engineering, Yildiz Campus, 34349, Besiktas, Istanbul, Turkey. E-mail: akbarov@yildiz.edu.tr (S. D. Akbarov)

² Institute of Mathematics and Mechanics of National Academy of Sciences of Azerbaijan, 37041, Baku, Azerbaijan.

³ Yildiz Technical University, Faculty of Chemical and Metallurgical Engineering Department of Mathematical Engineering, Davutpasa campus No 127, 34210 Esenler, Istanbul, Turkey.

⁴ Yildiz Technical University, Faculty of Civil Engineering, Department of Civil Engineering, Davutpasa campus No 127, 34210 Esenler, Istanbul, Turkey.

Keywords: Buckling delamination, critical strain, critical time, interface rectangular crack, sandwich rectangular plate, 3D FEM, viscoelastic material.

1 Introduction

One of the most common failure mechanisms in laminated composite materials is a local buckling around the delaminated zone, i.e. of the zone in which two adjacent layers are partially debonded at their interface.

Note that this zone may be formed as a consequence of various impact events, poor fabrication processes and fatigue. As is well known, the compressive strength of the structures made from laminated composite materials may be reduced several times by the presence of this delamination damage, which is modeled as a crack in the related research. The region bounded by a crack and the laminate free surface is liable to buckle locally under compressive loads, thereby creating conditions conducive to delamination growth and consequent global failure of the structure. One of the pioneer investigations related to the buckling-failure problem was made by Kachanov (1976) and numerous studies have so far been carried out in this field. A review of these investigations is given by Kardomateas, Pelgri and Malik (1995), Nilsson, Thesken, Sindelar, Giannakopoulos and Storakers (1993), Chai, Babcock and Knauss (1981), Wang, Cheng and Lin (1995) and others in which it is supposed that there is a crack which is parallel to the free plane and to the direction of the compressed external forces. In this case, the beginning of the delamination growing process is modeled as a buckling of the part of the material which occupies the region between the crack and the free plane and solutions are found in the framework of the approximate stability loss theories of plates or beams. It is evident that the results of these investigations do not apply in the cases where the thickness of this part is equal to or greater than the length of the crack. Moreover, there is a series of works, such as Hwang and Mao (1999), Short, Guild and Pavier (2001), Arman, Zor and Aksoy (2006), investigating the effects of the geometry of the delaminated portion on the buckling force of the laminate. At the same time, in these works the investigations were carried out experimentally and numerically with the use of the FEM modeling. For instance, in the paper by Hwang and Mao (1999), the influence of the delaminated zone (crack) on the global buckling critical forces of the plate-strip made from glass-fibre layers was studied. In the paper by Short, Guild and Pavier (2001), the effect of delamination geometry (i.e. the sizes of the rectangular interface crack) on the global buckling critical forces of the layered rectangular plate was investigated experimentally and numerically by employing 3D modeling using the packet programme ABAQUS V.5.8 FEM code. The same problem for the rectangular plate containing the circular cylindrical hole through the thickness of the plate was investigated by Arman, Zor and Aksoy (2006). It was

assumed that the circular delamination (crack) is around the circular hole and for obtaining numerical results 3D FEM modeling of the packet programme ANSYS 6.1 was used.

The buckling driven delaminations of compressed films and coatings on substrates were studied experimentally by Evans and Hutchinson (1995), Gioia and Ortiz (1997), Hutchinson and Suo (1992), Hutchinson et al. (1992), Nilsson and Giannakopoulos (1995), Thouless et al. (1994), Wang and Evans (1998), Moon et al. (2002). In these and in the other investigations of these authors (see, as an example, Moon et al (2004), Hutchinson et al. (2000)), the approximate mathematical modeling was also used for describing the experimentally studied problems. It should be noted that in all the foregoing investigations the fundamental buckling theories based on the three-dimensional nonlinear equations of the deformable body mechanics have not been proposed and used. Such theories, i.e. the Three-Dimensional Linearized Theory of Stability (TDLTS) of the deformable solid body mechanics for the local buckling problems for the bodies containing cracks was proposed and employed in the papers by Guz and Nazarenko (1985a, 1985b) and others. Note that a detailed description of the field equations and relations of the TDLTS are given in many references, for instance in the monograph by Guz (1999). A detailed description of some early results was given in the monograph by Guz (2008a, 2008b). The present level of these investigations is detailed in a paper of Bogdanov, Guz and Nazarenko (2009).

In all the investigations reviewed above it was assumed that the materials of the composites are time-independent. The development of the TDLTS based on the initial imperfection stability loss criterion by Hoff (1954) for the time dependent materials was proposed and employed in the works by Akbarov (1998, 2007), Akbarov, Sisman and Yahnioğlu (1997), Akbarov and Yahnioğlu (2001) and others. The description of some related results was also given in the monograph by Akbarov and Guz (2000). The development and application of the above-noted version of the TDLTS on the study of the buckling delamination problems of the elements of constructions (such as plate-strip, circular plate) fabricated from viscoelastic materials were made in the papers by Akbarov and Rzayev (2002a, 2002b, 2003), Rzayev and Akbarov (2002) and others. The review of these studies was considered in the paper by Akbarov (2007).

In these studies, the two-dimensional problems were analyzed for a plate-strip containing a crack whose edges are parallel to the face planes of the plate and a circular plate containing a penny-shaped crack the edge faces of which are also parallel to the plate's upper and lower face planes. Also, these investigations were carried out by utilizing 2D FEM modeling. In the present paper, however, an attempt is made to develop the approach proposed in the works by Akbarov and Rzayev (2002a,

2002b), Rzayev and Akbarov (2002) for the three-dimensional buckling delamination problems, namely, for the sandwich rectangular plate containing interface rectangular cracks. Two cases are considered; Case 1: It is assumed that the plate contains two interface embedded rectangular band cracks, Case 2: It is assumed that the plate contains two interface rectangular edge-cracks. For the concrete numerical investigation made by utilizing 3D FEM modeling, the material of the layers of the plates is modeled as homogeneous isotropic elastic and viscoelastic one.

2 Formulation of the problem

Consider a thick sandwich rectangular plate which contains two interface rectangular cracks. The Cartesian coordinate system $Ox_1x_2x_3$ is associated with the plate so as to give Lagrange coordinates of the points of the plate in the natural state. Assume that the plate occupies the region $V = V^{(r_1)} \cup V^{(r_2)} \cup V^{(r_3)}$ where $V^{(r_1)} = \{0 < x_1 < \ell_1; 0 < x_2 < h_F; 0 < x_3 < \ell_3\}$,

$$V^{(r_2)} = \{0 < x_1 < \ell_1; h_F < x_2 < h_F + h_C; 0 < x_3 < \ell_3\} \tag{1}$$

$$V^{(r_3)} = \{0 < x_1 < \ell_1; h_F + h_C < x_2 < h; 0 < x_3 < \ell_3\}$$

We will consider two cases with respect to the location of the cracks in the plate. In Case 1 we assume that the plate contains the two rectangular band-cracks (Fig. 1a), i.e. upper and lower interface band-cracks at

$$\Omega_1 = \{(\ell_1 - \ell_{10})/2 < x_1 < (\ell_1 + \ell_{10})/2; x_2 = h_F; 0 < x_3 < \ell_3\}$$

and

$$\Omega_2 = \{(\ell_1 - \ell_{10})/2 < x_1 < (\ell_1 + \ell_{10})/2; x_2 = h_F + h_C; 0 < x_3 < \ell_3\}. \tag{2}$$

But in Case 2 we assume that the plate contains two rectangular interface edge-cracks i.e. upper and lower interface edge-cracks at

$$\Omega'_1 = \{(\ell_1 - \ell_{10})/2 < x_1 < (\ell_1 + \ell_{10})/2; x_2 = h_F; 0 < x_3 < \ell_{30}\}$$

and

$$\Omega'_2 = \{(\ell_1 - \ell_{10})/2 < x_1 < (\ell_1 + \ell_{10})/2; x_2 = h_F + h_C; 0 < x_3 < \ell_{30}\}. \tag{3}$$

In equations (2) and (3) $\ell_{10}(\ell_{30})$ is the length of the cracks along the Ox_1 (Ox_3) axis. In Fig. 1 the face layers are indicated by the letter F , but the core layer is indicated

by the letter C . The meaning of the other notation used in Fig. 1 and in equations (1), (2) and (3) is obvious. Note that in Fig. 1 for clarity of the illustration one half (i.e. for $0 \leq x_1 \leq \ell_1$) of the plate is shown and the symmetry of the plate structure with respect to the plane $x_1 = \ell_1/2$ is taken into account.

We suppose that edge surfaces of the cracks have an initial infinitesimal imperfection and this imperfection is symmetric with respect to the $x_1 = \ell_1/2$ plane and with respect to the planes $x_2 = h_F$ (for the lower crack) and $x_2 = h_F + h_C$ (for the upper crack). The equations of the edge-surfaces of upper and lower cracks can be written as follows:

Case 1.

$$\begin{aligned} x_2^\pm &= h_F + \varepsilon f^\pm(x_1) \text{ (for the lower crack) and} \\ x_2^\pm &= h_F + h_C + \varepsilon f^\pm(x_1) \text{ (for the upper crack) for} \end{aligned}$$

$$(\ell_1 - \ell_{10})/2 < x_1 < (\ell_1 + \ell_{10})/2 \text{ and } 0 < x_3 < \ell_3 \quad (4)$$

and $f(x_1)$ satisfies the following relations,

$$\begin{aligned} f^+(x_1) &= -f^-(x_1), \\ f^\pm((\ell_1 - \ell_{10})/2) &= f^\pm((\ell_1 + \ell_{10})/2) = 0, \\ \frac{df^\pm((\ell_1 - \ell_{10})/2)}{dx_1} &= \frac{df^\pm((\ell_1 + \ell_{10})/2)}{dx_1} = 0 \end{aligned} \quad (5)$$

Case 2.

$$\begin{aligned} x_2^\pm &= h_F + \varepsilon f^\pm(x_1, x_3) \text{ (for the lower crack) and} \\ x_2^\pm &= h_F + h_C + \varepsilon f^\pm(x_1, x_3) \text{ (for the upper crack)} \\ \text{for} \end{aligned}$$

$$(\ell_1 - \ell_{10})/2 < x_1 < (\ell_1 + \ell_{10})/2 \text{ and } 0 \leq x_3 \leq \ell_{30} \quad (6)$$

and the function $f(x_1, x_3)$ satisfies the following relations.

$$\begin{aligned} f^+(x_1, x_3) &= -f^-(x_1, x_3), \\ f^\pm((\ell_1 - \ell_{10})/2, x_3) \Big|_{0 \leq x_3 \leq \ell_{30}} &= f^\pm((\ell_1 + \ell_{10})/2, x_3) \Big|_{0 \leq x_3 \leq \ell_{30}} = 0 \\ \frac{df^\pm((\ell_1 - \ell_{10})/2, x_3)}{dx_1} \Big|_{0 \leq x_3 \leq \ell_{30}} &= 0, \\ \frac{df^\pm((\ell_1 + \ell_{10})/2, x_3)}{dx_1} \Big|_{0 \leq x_3 \leq \ell_{30}} &= 0 \end{aligned}$$

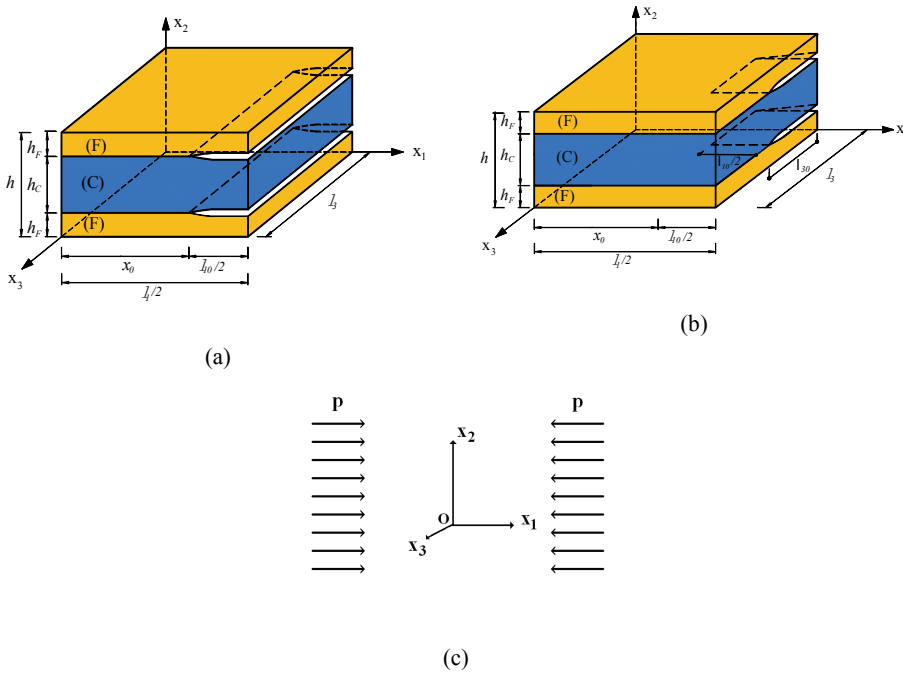


Figure 1: The geometry of the half part (for $0 \leq x_1 \leq l_1$) of the considered plate a) with band cracks (Case 1), b) with edge cracks (Case 2), c) the direction of initial forces.

$$f^\pm(x_1, l_{30}) \Big|_{(\ell_1 - \ell_{10})/2 < x_1 < (\ell_1 + \ell_{10})/2} = 0,$$

$$\frac{df^\pm(x_1, l_{30})}{dx_3} \Big|_{(\ell_1 - \ell_{10})/2 < x_1 < (\ell_1 + \ell_{10})/2} = 0. \tag{7}$$

In (4) and (6), ε is a dimensionless small parameter ($\varepsilon \ll 1$) which characterizes the degree of the initial imperfection of the crack edge-surfaces, h_F (h_C) is the thickness of the face-layers (the core layer) and the upper index “+” (“-”) represents the upper (lower) edge surface of the considered crack.

Thus, we investigate the evolution of the foregoing initial infinitesimal imperfections of the crack-edge surfaces under compression of the plate along the Ox_1 axis with uniformly distributed normal forces with intensity p (for the elastic plate) and as time elapses at the fixed value of the external compression force (for the viscoelastic plate). This evolution will be investigated by utilizing the three-dimensional geometrically nonlinear equations of the theory of viscoelasticity in the framework

of the piecewise homogeneous body model.

Below, the values relating the core layer and the face layers will be denoted by upper indices (1) and (2) respectively. At the same time, we will use upper index r_k ($k = 1, 2, 3$) where r_1 and r_3 indicate the values related to lower and upper layers, respectively, but r_2 indicates the values related to the core layer, so that $r_1 = r_3 = 2$, $r_2 = 1$. It is assumed that the face layers of the sandwich plate are made from the same materials and the structure of the plate is symmetric with respect to the middle plane of the core layer.

Within the framework of the three dimensional geometrically nonlinear equations of the theory of elasticity the governing field equations are

Equilibrium equation

$$\frac{\partial}{\partial x_j} \left[\sigma_{jn}^{(r_k)} \left(\delta_i^n + \frac{\partial u_i^{(r_k)}}{\partial x_n} \right) \right] = 0, \quad i, j, n; k = 1, 2, 3,$$

$$r_1 = r_3 = 2, \quad r_2 = 1 \quad (8)$$

Geometrical relation

$$\varepsilon_{ij}^{(r_k)} = \frac{1}{2} \left(\frac{\partial u_i^{(r_k)}}{\partial x_j} + \frac{\partial u_j^{(r_k)}}{\partial x_i} + \frac{\partial u_n^{(r_k)}}{\partial x_i} \frac{\partial u_n^{(r_k)}}{\partial x_j} \right), \quad (9)$$

Constitutive relation

$$\sigma_{ij}^{(r_k)} = \lambda^{*(r_k)} \theta^{(r_k)} \delta_i^j + 2\mu^{*(r_k)} \varepsilon_{ij}^{(r_k)},$$

$$\theta^{(r_k)} = \varepsilon_{11}^{(r_k)} + \varepsilon_{22}^{(r_k)} + \varepsilon_{33}^{(r_k)}, \quad (10)$$

where $\lambda^{*(r_k)}$ and $\mu^{*(r_k)}$ are the following operators

$$\lambda^{*(r_k)} \phi(t) = \lambda_0^{(r_k)} \phi(t) + \int_0^t \lambda^{(r_k)}(t - \tau) \phi(\tau) d\tau,$$

$$\mu^{*(r_k)} \phi(t) = \mu_0^{(r_k)} \phi(t) + \int_0^t \mu^{(r_k)}(t - \tau) \phi(\tau) d\tau. \quad (11)$$

In equations (8)-(12) the conventional notation is used. Consider the formulation of the boundary and contact conditions for Case 1 and Case 2 separately.

Case 1.

Boundary conditions at the ends of the plate:

$$\begin{aligned}
 u_2^{(r_k)} \Big|_{x_1=0;\ell_1} &= 0, & u_2^{(r_k)} \Big|_{x_3=0;\ell_3} &= 0, \\
 \left[\sigma_{1n}^{(r_k)} \left(\delta_1^n + \frac{\partial u_1^{(r_k)}}{\partial x_n} \right) \right] \Big|_{x_1=0;\ell_1} &= p, \\
 \left[\sigma_{1n}^{(r_k)} \left(\delta_3^n + \frac{\partial u_3^{(r_k)}}{\partial x_n} \right) \right] \Big|_{x_1=0;\ell_1} &= 0, \\
 \left[\sigma_{3n}^{(r_k)} \left(\delta_1^n + \frac{\partial u_1^{(r_k)}}{\partial x_n} \right) \right] \Big|_{x_3=0;\ell_3} &= 0, \\
 \left[\sigma_{3n}^{(r_k)} \left(\delta_3^n + \frac{\partial u_3^{(r_k)}}{\partial x_n} \right) \right] \Big|_{x_3=0;\ell_3} &= 0
 \end{aligned} \tag{12}$$

Boundary conditions on the free face planes of the plate:

$$\begin{aligned}
 \left[\sigma_{2n}^{(r_1)} \left(\delta_i^n + \frac{\partial u_i^{(r_1)}}{\partial x_n} \right) \right] \Big|_{x_2=0} &= 0, \\
 \left[\sigma_{2n}^{(r_3)} \left(\delta_i^n + \frac{\partial u_i^{(r_3)}}{\partial x_n} \right) \right] \Big|_{x_2=h} &= 0
 \end{aligned} \tag{13}$$

Boundary conditions on the cracks' edge surfaces

$$\begin{aligned}
 \left[\sigma_{jn}^{(r_1)} \left(\delta_i^n + \frac{\partial u_i^{(r_1)}}{\partial x_n} \right) \right] \Big|_{S_1^-} n_j^- &= 0, \\
 \left[\sigma_{jn}^{(r_2)} \left(\delta_i^n + \frac{\partial u_i^{(r_2)}}{\partial x_n} \right) \right] \Big|_{S_1^+} n_j^+ &= 0, \\
 \left[\sigma_{jn}^{(r_3)} \left(\delta_i^n + \frac{\partial u_i^{(r_3)}}{\partial x_n} \right) \right] \Big|_{S_2^+} n_j^+ &= 0, \\
 \left[\sigma_{jn}^{(r_2)} \left(\delta_i^n + \frac{\partial u_i^{(r_2)}}{\partial x_n} \right) \right] \Big|_{S_2^-} n_j^- &= 0,
 \end{aligned}$$

$$\begin{aligned}
\mathcal{S}_1^\pm &= \{((\ell_1 - \ell_{10})/2 < x_1 < (\ell_1 + \ell_{10})/2), \\
x_2^\pm &= h_F + \varepsilon f^\pm(x_1), 0 < x_3 < \ell_3\}, \\
\mathcal{S}_2^\pm &= \{((\ell_1 - \ell_{10})/2 < x_1 < (\ell_1 + \ell_{10})/2), \\
x_2^\pm &= h_F + h_C + \varepsilon f^\pm(x_1), 0 < x_3 < \ell_3\}
\end{aligned} \tag{14}$$

Contact conditions between the layers of the plate:

$$\begin{aligned}
u_i^{(r_1)} \Big|_{\mathcal{D}_1^-} &= u_i^{(r_2)} \Big|_{\mathcal{D}_1^+}, \quad u_i^{(r_3)} \Big|_{\mathcal{D}_2^+} = u_i^{(r_2)} \Big|_{\mathcal{D}_2^-}, \\
\left[\sigma_{2n}^{(r_1)} \left(\delta_i^n + \frac{\partial u_i^{(r_1)}}{\partial x_n} \right) \right] \Big|_{\mathcal{D}_1^-} &= \left[\sigma_{2n}^{(r_2)} \left(\delta_i^n + \frac{\partial u_i^{(r_2)}}{\partial x_n} \right) \right] \Big|_{\mathcal{D}_1^+}, \\
\left[\sigma_{2n}^{(r_3)} \left(\delta_i^n + \frac{\partial u_i^{(r_3)}}{\partial x_n} \right) \right] \Big|_{\mathcal{D}_2^+} &= \left[\sigma_{2n}^{(r_2)} \left(\delta_i^n + \frac{\partial u_i^{(r_2)}}{\partial x_n} \right) \right] \Big|_{\mathcal{D}_2^-}, \\
\mathcal{D}_1^\pm &= \{x_1 \in ((0, (\ell_1 - \ell_{10})/2) \cup ((\ell_1 + \ell_{10})/2, \ell_1)), \\
x_2 &= h_F \pm 0, x_3 \in (0, \ell_3)\}, \\
\mathcal{D}_2^\pm &= \{x_1 \in ((0, (\ell_1 - \ell_{10})/2) \cup ((\ell_1 + \ell_{10})/2, \ell_1)), \\
x_2 &= h_F + h_C \pm 0, x_3 \in (0, \ell_3)\}.
\end{aligned} \tag{15}$$

Case 2.

Boundary conditions at the ends of the plate:

$$\begin{aligned}
u_2^{(r_k)} \Big|_{x_1=0; \ell_1} &= 0, \quad u_2^{(r_k)} \Big|_{x_3=\ell_3} = 0, \\
\left[\sigma_{1n}^{(r_k)} \left(\delta_1^n + \frac{\partial u_1^{(r_k)}}{\partial x_n} \right) \right] \Big|_{x_1=0; \ell_1} &= p, \\
\left[\sigma_{1n}^{(r_k)} \left(\delta_3^n + \frac{\partial u_3^{(r_k)}}{\partial x_n} \right) \right] \Big|_{x_1=0; \ell_1} &= 0, \\
\left[\sigma_{3n}^{(r_k)} \left(\delta_1^n + \frac{\partial u_1^{(r_k)}}{\partial x_n} \right) \right] \Big|_{x_3=\ell_3} &= 0, \\
\left[\sigma_{3n}^{(r_k)} \left(\delta_3^n + \frac{\partial u_3^{(r_k)}}{\partial x_n} \right) \right] \Big|_{x_3=\ell_3} &= 0,
\end{aligned}$$

$$\left[\sigma_{3n}^{(r_k)} \left(\delta_i^n + \frac{\partial u_i^{(r_k)}}{\partial x_n} \right) \right] \Big|_{x_3=0} = 0 \tag{16}$$

Boundary conditions on the free face planes of the plate:

$$\begin{aligned} \left[\sigma_{2n}^{(r_1)} \left(\delta_i^n + \frac{\partial u_i^{(r_1)}}{\partial x_n} \right) \right] \Big|_{x_2=0} &= 0, \\ \left[\sigma_{2n}^{(r_3)} \left(\delta_i^n + \frac{\partial u_i^{(r_3)}}{\partial x_n} \right) \right] \Big|_{x_2=h} &= 0. \end{aligned} \tag{17}$$

Boundary conditions on the cracks' edge surfaces:

$$\begin{aligned} \left[\sigma_{jn}^{(r_1)} \left(\delta_i^n + \frac{\partial u_i^{(r_1)}}{\partial x_n} \right) \right] \Big|_{S_3^-} n_j^- &= 0, \\ \left[\sigma_{jn}^{(r_2)} \left(\delta_i^n + \frac{\partial u_i^{(r_2)}}{\partial x_n} \right) \right] \Big|_{S_3^+} n_j^+ &= 0, \\ \left[\sigma_{jn}^{(r_3)} \left(\delta_i^n + \frac{\partial u_i^{(r_3)}}{\partial x_n} \right) \right] \Big|_{S_4^+} n_j^+ &= 0, \\ \left[\sigma_{jn}^{(r_2)} \left(\delta_i^n + \frac{\partial u_i^{(r_2)}}{\partial x_n} \right) \right] \Big|_{S_4^-} n_j^- &= 0, \end{aligned}$$

$$\begin{aligned} S_3^\pm &= \{ ((\ell_1 - \ell_{10})/2 < x_1 < (\ell_1 + \ell_{10})/2), \\ x_2^\pm &= h_F + \epsilon f^\pm(x_1, x_3), 0 < x_3 < \ell_{30} \}, \\ S_4^\pm &= \{ ((\ell_1 - \ell_{10})/2 < x_1 < (\ell_1 + \ell_{10})/2), \\ x_2^\pm &= h_F + h_C + \epsilon f^\pm(x_1, x_3), 0 < x_3 < \ell_{30} \}. \end{aligned} \tag{18}$$

Contact conditions between the layers of the plate:

$$\begin{aligned} u_i^{(r_1)} \Big|_{\varnothing_1^-} &= u_i^{(r_2)} \Big|_{\varnothing_1^+} \quad u_i^{(r_3)} \Big|_{\varnothing_2^+} = u_i^{(r_2)} \Big|_{\varnothing_2^-}, \\ \left[\sigma_{2n}^{(r_1)} \left(\delta_i^n + \frac{\partial u_i^{(r_1)}}{\partial x_n} \right) \right] \Big|_{\varnothing_1^-} &= \left[\sigma_{2n}^{(r_2)} \left(\delta_i^n + \frac{\partial u_i^{(r_2)}}{\partial x_n} \right) \right] \Big|_{\varnothing_1^+}, \end{aligned}$$

$$\begin{aligned}
 & \left[\sigma_{2n}^{(r_3)} \left(\delta_i^n + \frac{\partial u_i^{(r_3)}}{\partial x_n} \right) \right] \Big|_{\wp_2^+} = \left[\sigma_{2n}^{(r_2)} \left(\delta_i^n + \frac{\partial u_i^{(r_2)}}{\partial x_n} \right) \right] \Big|_{\wp_2^-}, \\
 & u_i^{(r_1)} \Big|_{\wp_3^-} = u_i^{(r_2)} \Big|_{\wp_3^+}, \quad u_i^{(r_3)} \Big|_{\wp_4^+} = u_i^{(r_2)} \Big|_{\wp_4^-}, \\
 & \left[\sigma_{2n}^{(r_1)} \left(\delta_i^n + \frac{\partial u_i^{(r_1)}}{\partial x_n} \right) \right] \Big|_{\wp_3^-} = \left[\sigma_{2n}^{(r_2)} \left(\delta_i^n + \frac{\partial u_i^{(r_2)}}{\partial x_n} \right) \right] \Big|_{\wp_3^+}, \\
 & \left[\sigma_{2n}^{(r_3)} \left(\delta_i^n + \frac{\partial u_i^{(r_3)}}{\partial x_n} \right) \right] \Big|_{\wp_4^+} = \left[\sigma_{2n}^{(r_2)} \left(\delta_i^n + \frac{\partial u_i^{(r_2)}}{\partial x_n} \right) \right] \Big|_{\wp_4^-}, \\
 & \wp_3^\pm = \{(\ell_1 - \ell_{10})/2 \leq x_1 \leq (\ell_1 + \ell_{10})/2, \\
 & x_2 = h_F \pm 0, \ell_{30} < x_3 < \ell_3\}, \\
 & \wp_4^\pm = \{(\ell_1 - \ell_{10})/2 \leq x_1 \leq (\ell_1 + \ell_{10})/2, \\
 & x_2 = h_F + h_C \pm 0, \ell_{30} < x_3 < \ell_3\}, \tag{19}
 \end{aligned}$$

where n_j (n_j^\pm) in equations (15) and (19) is the orthonormal components of the unit normal vector of the considered surfaces (i.e. acting on the cracks' edge surfaces). The other notation used in Eqs. (8)-(20) is conventional.

Having thus completed the formulation of the considered problem now we consider the method of solution.

3 Solution procedure

To simplify the analysis we consider only the solution procedure for Case 2 from which as a particular case, the solution procedure for Case 1 can be obtained. First, using the equations of the crack edge surfaces given in (6), the equation $x_2^\pm = h_F + \epsilon f^\pm(x_1, x_3)$ or $x_2^\pm = h_F + h_C + \epsilon f^\pm(x_1, x_3)$

we derive the following expressions for n_j^\pm :

$$\begin{aligned}
 n_1^\pm &= \frac{\pm \epsilon \frac{\partial f^\pm(x_1, x_3)}{\partial x_1}}{\sqrt{1 + \epsilon^2 \left(\frac{\partial f^\pm(x_1, x_3)}{\partial x_1} \right)^2 + \epsilon^2 \left(\frac{\partial f^\pm(x_1, x_3)}{\partial x_3} \right)^2}}, \\
 n_2^\pm &= \frac{\pm 1}{\sqrt{1 + \epsilon^2 \left(\frac{\partial f^\pm(x_1, x_3)}{\partial x_1} \right)^2 + \epsilon^2 \left(\frac{\partial f^\pm(x_1, x_3)}{\partial x_3} \right)^2}},
 \end{aligned}$$

$$n_3^\pm = \frac{\pm \varepsilon \frac{\partial f^\pm(x_1, x_3)}{\partial x_3}}{\sqrt{1 + \varepsilon^2 \left(\frac{\partial f^\pm(x_1, x_3)}{\partial x_1} \right)^2 + \varepsilon^2 \left(\frac{\partial f^\pm(x_1, x_3)}{\partial x_3} \right)^2}}. \tag{20}$$

Note that the expression (21) occurs for the surfaces S_3^\pm and S_4^\pm (19) simultaneously.

Assume that $\varepsilon^2 \left[\left(\frac{\partial f^\pm(x_1, x_3)}{\partial x_1} \right)^2 + \left(\frac{\partial f^\pm(x_1, x_3)}{\partial x_3} \right)^2 \right] \leq 1$ according to which, the expression (21) can be represented in the series form in terms of the small parameter ε :

$$n_1^\pm = \sum_{k=0}^{\infty} \varepsilon^{2k+1} n_{1k}^\pm(x_1, x_3), \quad n_2^\pm = \pm 1 + \sum_{k=1}^{\infty} \varepsilon^{2k} n_{2k}^\pm(x_1, x_3),$$

$$n_3^\pm = \sum_{k=0}^{\infty} \varepsilon^{2k+1} n_{3k}^\pm(x_1, x_3). \tag{21}$$

In equation (22), the explicit expressions of the coefficients $n_{1k}^\pm(x_1, x_3)$, $n_{2k}^\pm(x_1, x_3)$ and $n_{3k}^\pm(x_1, x_3)$ are too long so they are not given here. At the same time, these expressions can be easily attained by employing the well known power series expansion of the expressions given in (21). Note that the equations (21) and (22) are written for Case 2 and by substituting $\partial f / \partial x_3 = 0$ we get the corresponding expressions for Case 1. According to Akbarov (1998), Akbarov and Yahnioglu (2001), Akbarov, Sisman and Yahnioglu (1997), Akbarov and Rzayev (2002a, 2002b, 2003), Rzayev and Akbarov (2002), the sought values are represented in series form in terms of ε as follows,

$$\left\{ \sigma_{ij}^{(r_k)}; \varepsilon_{ij}^{(r_k)}; u_i^{(r_k)} \right\} = \sum_{q=0}^{\infty} \varepsilon^q \left\{ \sigma_{ij}^{(r_k), q}; \varepsilon_{ij}^{(r_k), q}; u_i^{(r_k), q} \right\}. \tag{22}$$

After substituting equation (23) into equations (8), (9) and (10) and comparing identical powers of ε , we obtain the corresponding closed system of equations and boundary conditions to describe each approximation. Owing to the linearity of mechanical relations in equation (10) and the end conditions for displacements in equations (18) and (20), these relations and conditions will be satisfied for each approximation Eq. (23) separately. The remaining relations obtained from equations (8), (9) and (10) for every q -th approximation contains the values of all the previous approximations. At the same time, under satisfying the boundary conditions on the crack' edge surfaces, i.e. the conditions in equation (19) we employ the boundary form perturbation technique, according to which, the values of each approximation Eq. (23) related the core layer are expanded in series in the vicinity of $(x_1, h_F + 0, x_3)$ and $(x_1, h_F + h_C - 0, x_3)$, but the values of each approximation Eq. (23) related the upper face (lower face) layer in the vicinity $(x_1, h_F + h_C + 0, x_3)$

(in the vicinity $(x_1, h_F - 0, x_3)$), and using the expression (22) the corresponding conditions on the crack edge surfaces are also obtained for the first and subsequent approximations.

It follows from the well-known mechanical considerations that for the comparatively rigid composites under determination of the zeroth approximation we can use the relation $\delta_i^n + \frac{\partial u_i^{(0)}}{\partial x_n} \approx \delta_i^n$ according to which the field equations and boundary and contact conditions attained from Eqs. (8)-(20) for the zeroth approximation coincide with the corresponding ones of the classical linear theory for viscoelastic bodies. In this case for determination of the values related the zeroth approximation we use the principle of correspondence by using the Laplace transform

$$\bar{\varphi}(s) = \int_0^\infty \varphi(t)e^{-st} dt \tag{23}$$

with the parameter $s > 0$. So, replacing $\sigma_{ij}^{(r_k),1}$, $\epsilon_{ij}^{(r_k),1}$, $u_i^{(r_k),1}$, $\lambda^{(r_k)}$ and $\mu^{(r_k)}$ in the corresponding equations and relations by $\bar{\sigma}_{ij}^{(r_k),1}$, $\bar{\epsilon}_{ij}^{(r_k),1}$, $\bar{u}_i^{(r_k),1}$, $\bar{\lambda}^{(r_k)}$ and $\bar{\mu}^{(r_k)}$ respectively, we obtain the field equations, boundary and contact conditions for the Laplace transform of the values of the zeroth approximation. It is evident that, according to the nonhomogeneity of the plate material under the action of the uniformly distributed normal forces with intensity p at the ends of the plate the inhomogeneous distribution of the stresses and strains applies in the layers. But, these inhomogeneous distributions arise only in the very near vicinity of the ends of the plate and does not influence the local buckling delamination of the plate parts around the rectangular cracks. Therefore, we do not take the mentioned inhomogeneous distribution of the stresses and strains into account under determination of the values of the zeroth approximation. Thus, using the relations $2h_F\sigma_{11}^{(2),0}(t) + h_C\sigma_{11}^{(1),0}(t) = ph$ and $\sigma_{11}^{(2),0}(t)/E^{*(2)} = \sigma_{11}^{(1),0}(t)/E^{*(1)}$ (where $E^{*(k)}\phi(t) = E_0^{(k)}\phi(t) + \int_0^t E^{(k)}(t-\tau)\phi(\tau)d\tau$, and $E_0^{(k)}$ is an instantaneous value of a modulus of elasticity of the (r_k) -th material) we can write the following expressions for the Laplace transform of the zeroth approximation

$$\begin{aligned} \bar{\sigma}_{11}^{(r_1),0} = \bar{\sigma}_{11}^{(r_3),0} &= p \frac{\bar{E}^{*(2)}(2h_F + h_C)}{s2\bar{E}^{*(1)}h_F + \bar{E}^{*(2)}h_C}, \\ \bar{\sigma}_{11}^{(r_2),0} &= \bar{\sigma}_{11}^{(r_1),0} \frac{\bar{E}^{*(1)}}{\bar{E}^{*(2)}}, \quad \bar{\sigma}_{ij}^{(r_k),0} = 0 \text{ for } ij \neq 11. \end{aligned} \tag{24}$$

Selecting the suitable expression for the core function $E^{(k)}(t)$ of the integral operator $E^{*(k)}$ and employing some algorithm for calculation of the inverse Laplace

transform we can determine the stresses

$$\sigma_{11}^{(r_k),0} = \sigma_{11}^{(r_k),0}(t), \quad \sigma_{ij}^{(r_k),0} = 0 \text{ for } ij \neq 11, \quad (25)$$

related with the zeroth approximation.

Now we consider the determination of the values of the first approximation. According to the foregoing assumptions (25) and (26) we obtain the following equilibrium equations, mechanical and geometrical relations for the first approximation.

$$\begin{aligned} \frac{\partial \sigma_{ji}^{(r_k),1}}{\partial x_j} + \sigma_{11}^{(r_k),0}(t) \frac{\partial^2 u_i^{(r_k),1}}{\partial x_1^2} &= 0, \\ \sigma_{ij}^{(r_k),1} &= \lambda^{*(r_k)} \theta^{(r_k),1} \delta_i^j + 2\mu^{*(r_k)} \varepsilon_{ij}^{(r_k),1}, \\ \varepsilon_{ij}^{(r_k),1} &= \frac{1}{2} \left(\frac{\partial u_i^{(r_k),1}}{\partial x_j} + \frac{\partial u_j^{(r_k),1}}{\partial x_i} \right). \end{aligned} \quad (26)$$

Consider the boundary and contact conditions attained for the first approximation related Case 2.

Boundary conditions at the ends of the plate:

$$\begin{aligned} u_2^{(r_k),1} \Big|_{x_1=0;\ell_1} &= 0, \quad u_2^{(r_k),1} \Big|_{x_3=\ell_3} = 0, \\ \left[\sigma_{11}^{(r_k),1} + \sigma_{11}^{(r_k),0}(t) \frac{\partial u_1^{(r_k),1}}{\partial x_n} \right] \Big|_{x_1=0;\ell_1} &= 0, \\ \sigma_{13}^{(r_k),1} \Big|_{x_1=0;\ell_1} &= 0, \\ \sigma_{31}^{(r_k),1} \Big|_{x_3=\ell_3} &= \sigma_{33}^{(r_k),1} \Big|_{x_3=\ell_3} = 0, \\ \sigma_{31}^{(r_k),1} \Big|_{x_3=0} &= \sigma_{32}^{(r_k),1} \Big|_{x_3=0} = \sigma_{33}^{(r_k),1} \Big|_{x_3=0} = 0. \end{aligned} \quad (27)$$

Boundary conditions on the free face planes of the plate:

$$\begin{aligned} \sigma_{21}^{(r_1),1} \Big|_{x_2=0} &= \sigma_{22}^{(r_1),1} \Big|_{x_2=0} = \sigma_{23}^{(r_1),1} \Big|_{x_2=0} = 0, \\ \sigma_{21}^{(r_3),1} \Big|_{x_2=h} &= \sigma_{22}^{(r_3),1} \Big|_{x_2=h} = \sigma_{23}^{(r_3),1} \Big|_{x_2=h} = 0. \end{aligned} \quad (28)$$

Boundary conditions on the cracks' edge surfaces:

$$\begin{aligned}
\sigma_{21}^{(r_1),1} \Big|_{\bar{s}_3^-} &= -\sigma_{11}^{(r_1),0}(t) \frac{\partial f^-}{\partial x_1}, \\
\sigma_{22}^{(r_1),1} \Big|_{\bar{s}_3^-} &= \sigma_{23}^{(r_1),1} \Big|_{\bar{s}_3^-} = 0, \quad \sigma_{21}^{(r_2),1} \Big|_{\bar{s}_3^+} = -\sigma_{11}^{(r_2),0}(t) \frac{\partial f^+}{\partial x_1}, \\
\sigma_{22}^{(r_2),1} \Big|_{\bar{s}_3^+} &= \sigma_{23}^{(r_2),1} \Big|_{\bar{s}_3^+} = 0, \\
\sigma_{21}^{(r_2),1} \Big|_{\bar{s}_4^-} &= -\sigma_{11}^{(r_2),0}(t) \frac{\partial f^-}{\partial x_1}, \quad \sigma_{22}^{(r_2),1} \Big|_{\bar{s}_4^-} = \sigma_{23}^{(r_2),1} \Big|_{\bar{s}_4^-} = 0, \\
\sigma_{21}^{(r_3),1} \Big|_{\bar{s}_4^+} &= -\sigma_{11}^{(r_3),0}(t) \frac{\partial f^+}{\partial x_1}, \\
\sigma_{22}^{(r_3),1} \Big|_{\bar{s}_4^+} &= \sigma_{23}^{(r_3),1} \Big|_{\bar{s}_4^+} = 0, \\
\bar{s}_3^\pm &= \{((\ell_1 - \ell_{10})/2 < x_1 < (\ell_1 + \ell_{10})/2)\}, \\
x_2^\pm &= h_F \pm 0, 0 < x_3 < \ell_{30}\}, \\
\bar{s}_4^\pm &= \{((\ell_1 - \ell_{10})/2 < x_1 < (\ell_1 + \ell_{10})/2)\}, \\
x_2^\pm &= h_F + h_C \pm 0, 0 < x_3 < \ell_{30}\} \tag{29}
\end{aligned}$$

Contact conditions between the layers of the plate:

$$\begin{aligned}
u_i^{(r_1),1} \Big|_{\varrho_1^-} &= u_i^{(r_2),1} \Big|_{\varrho_1^+}, \quad u_i^{(r_3),1} \Big|_{\varrho_2^+} = u_i^{(r_2),1} \Big|_{\varrho_2^-}, \\
\left[\sigma_{21}^{(r_1),1} + \sigma_{11}^{(r_1),0}(t) \frac{\partial u_i^{(r_1),1}}{\partial x_1} \right] \Big|_{\varrho_1^-} &= \left[\sigma_{21}^{(r_2),1} + \sigma_{11}^{(r_2),0}(t) \frac{\partial u_i^{(r_2),1}}{\partial x_1} \right] \Big|_{\varrho_1^+}, \\
\sigma_{22}^{(r_1),1} \Big|_{\varrho_1^-} &= \sigma_{22}^{(r_2),1} \Big|_{\varrho_1^+}, \quad \sigma_{23}^{(r_1),1} \Big|_{\varrho_1^-} = \sigma_{23}^{(r_2),1} \Big|_{\varrho_1^+}, \\
\left[\sigma_{21}^{(r_3),1} + \sigma_{11}^{(r_3),0}(t) \frac{\partial u_i^{(r_3),1}}{\partial x_1} \right] \Big|_{\varrho_2^+} &= \left[\sigma_{21}^{(r_2),1} + \sigma_{11}^{(r_2),0}(t) \frac{\partial u_i^{(r_2),1}}{\partial x_1} \right] \Big|_{\varrho_2^-}, \\
\sigma_{22}^{(r_3),1} \Big|_{\varrho_2^+} &= \sigma_{22}^{(r_2),1} \Big|_{\varrho_2^-}, \quad \sigma_{23}^{(r_3),1} \Big|_{\varrho_2^+} = \sigma_{23}^{(r_2),1} \Big|_{\varrho_2^-}, \\
u_i^{(r_1),1} \Big|_{\varrho_3^-} &= u_i^{(r_2),1} \Big|_{\varrho_3^+}, \quad u_i^{(r_3),1} \Big|_{\varrho_4^+} = u_i^{(r_2),1} \Big|_{\varrho_4^-},
\end{aligned}$$

$$\begin{aligned}
 & \left[\sigma_{21}^{(r_1),1} + \sigma_{11}^{(r_1),0}(t) \frac{\partial u_i^{(r_1),1}}{\partial x_1} \right] \Big|_{\varrho_3^-} = \left[\sigma_{21}^{(r_2),1} + \sigma_{11}^{(r_2),0}(t) \frac{\partial u_i^{(r_2),1}}{\partial x_1} \right] \Big|_{\varrho_3^+}, \\
 & \sigma_{22}^{(r_1),1} \Big|_{\varrho_3^-} = \sigma_{22}^{(r_2),1} \Big|_{\varrho_3^+}, \quad \sigma_{23}^{(r_1),1} \Big|_{\varrho_3^-} = \sigma_{23}^{(r_2),1} \Big|_{\varrho_3^+}, \\
 & \left[\sigma_{21}^{(r_3),1} + \sigma_{11}^{(r_3),0}(t) \frac{\partial u_i^{(r_3),1}}{\partial x_1} \right] \Big|_{\varrho_4^+} = \left[\sigma_{21}^{(r_2),1} + \sigma_{11}^{(r_2),0}(t) \frac{\partial u_i^{(r_2),1}}{\partial x_1} \right] \Big|_{\varrho_4^-}, \\
 & \sigma_{22}^{(r_3),1} \Big|_{\varrho_4^+} = \sigma_{22}^{(r_2),1} \Big|_{\varrho_4^-}, \quad \sigma_{23}^{(r_3),1} \Big|_{\varrho_4^+} = \sigma_{23}^{(r_2),1} \Big|_{\varrho_4^-}. \tag{30}
 \end{aligned}$$

This completes the formulation of the boundary value problem corresponding to the first approximation.

In a likewise manner the corresponding equations and boundary conditions for the second and subsequent approximations can also be obtained. Thus, the investigation of buckling delamination around an interface rectangular crack contained within a sandwich rectangular plate is reduced to the solutions to series-boundary value problems such as (27)-(31). As in papers by Akbarov and Rzayev (2002a, 2002b, 2003) and others, by direct verification it is proven that the linear equations in (27)-(31) coincide with the corresponding equations for TDLTS presented by Guz (1999).

After the determination of the stress-deformation state in the considered plate (using the solution procedure described above) it is necessary to select the stability loss criteria. According to Hoff (1954), for the stability loss criterion we will assume that the case where the size of the initial imperfection starts to increase and grows indefinitely with the external compressive forces (for the elastic plate) or with duration of time (for the viscoelastic plate) under considerable fixed finite values of these forces. From this criterion the critical force or the critical time will be determined.

The investigations which are not detailed here indicate that the values of the critical force or of the critical time can be determined only within the framework of the zeroth and the first approximations. The second and the subsequent approximations do not change the values of the critical parameters. Taking these subsequent approximations into account improves only the accuracy of the stress distributions in the plate. Since our aim is to investigate the stability loss (i.e. to determine the values of the critical parameters), we restrict ourselves with the consideration of the zeroth and the first approximations.

According to the foregoing considerations, the stresses in the zeroth approximation have already been determined by the expressions (25) and (26). Now we consider

the determination of the values of the first approximation for which it is necessary to solve the problem (27)-(31). For this purpose, as under the determination of the zeroth approximation, we attempt to use the principle of correspondence by using the Laplace transform (24). It should be noted that under this procedure the following difficulty arises. In the equation (27) and in the conditions (28) and (31) $\sigma_{11}^{(r_k),0}(t)$, as it has been noted above, depends on time and therefore the Laplace transform of the term $\sigma_{11}^{(r_k),0}(t) \partial^2 u_i^{(r_k),1} / \partial x_1^2$ in equation (27) and the Laplace transform of the term $\sigma_{11}^{(r_k),0}(t) \partial u_i^{(r_k),1} / \partial x_1$ in the conditions (28) and (31) can not be written as $\bar{\sigma}_{11}^{(r_k),0} \partial^2 \bar{u}_i^{(r_k),1} / \partial x_1^2$ and as $\bar{\sigma}_{11}^{(r_k),0} \partial \bar{u}_i^{(r_k),1} / \partial x_1$, respectively. To overcome this difficulty we assume that $\sigma_{11}^{(r_k),0}(t)$ varies slowly in time and takes value of $\sigma_{11}^{(r_k),0}(t)$ at some fixed moment $t = t_1$ and consequently, instead of Laplace transform of the terms $\sigma_{11}^{(r_k),0}(t) \partial^2 u_i^{(r_k),1} / \partial x_1^2$ and $\sigma_{11}^{(r_k),0}(t) \partial u_i^{(r_k),1} / \partial x_1$ to write $\sigma_{11}^{(r_k),0}(t_1) \partial^2 \bar{u}_i^{(r_k),1} / \partial x_1^2$ and $\sigma_{11}^{(r_k),0}(t_1) \partial \bar{u}_i^{(r_k),1} / \partial x_1$, respectively. This assumption, also used in the papers by Rzayev (2002), Rzayev and Akbarov (2002), Akbarov and Yahnioglu (2001), allows us to obtain accurate results if the variation of $\sigma_{11}^{(r_k),0}$ with respect to time is insignificant. Thus, taking the foregoing discussions into account and replacing $\sigma_{ij}^{(k),1}$, $\varepsilon_{ij}^{(k),1}$, $u_i^{(k),1}$, $\sigma_{11}^{(r_k),0}(t)$, $\lambda^{(k)}$ and $\mu^{(k)}$ in (27)-(31) by $\bar{\sigma}_{ij}^{(k),1}$, $\bar{\varepsilon}_{ij}^{(k),1}$, $\bar{u}_i^{(k),1}$, $\sigma_{11}^{(r_k),0}(t_1)$, $\bar{\lambda}^{*(k)}$ and $\bar{\mu}^{*(k)}$ respectively, we obtain the corresponding equations and boundary conditions with respect to the Laplace transform of values for the first approximation. For the solution to the problems corresponding to the Laplace transforms of the sought values we employ the Finite Element Method (FEM).

4 FEM modeling of the considered problems

FEM analysis is widely used for the solution to various problems in branches of engineering and sciences. The present level of FEM modeling was presented and analyzed by Atluri (2005), Alaimo, Milazzo and Orlando (2008), Attaporn and Koguchi (2009) and many others. As it follows from the listed references that for FEM modeling by employing the Ritz method it is necessary to construct the functional, the Euler equation of which are the equations (27)-(31) rewritten for the Laplace transform of the corresponding sought functions. For the realization of this construction the equations (27)-(31) must be self-adjoint ones. In monograph by Guz (1999) it is proven that the equations of the TDLTS are the self-adjoint. According to this statement, we construct the following functional for the problems under consideration.

In Case 2 the equations (27)-(31) for the Laplace transform of the sought functions

are the Euler equations of the following functional.

$$\begin{aligned}
 \Pi \left(\bar{u}_1^{(r_k),1}, \bar{u}_2^{(r_k),1}, \bar{u}_3^{(r_k),1} \right) = & \\
 \sum_{k=1}^3 \left[\frac{1}{2} \iiint_{V^{(r_k)}} \left[\left(\bar{\sigma}_{11}^{(r_k),1} + \sigma_{11}^{(r_k),0}(t_1) \frac{\partial \bar{u}_1^{(r_k),1}}{\partial x_1} \right) \frac{\partial \bar{u}_1^{(r_k),1}}{\partial x_1} + \right. & \\
 \bar{\sigma}_{12}^{(r_k),1} \frac{\partial \bar{u}_1^{(r_k),1}}{\partial x_2} + \bar{\sigma}_{13}^{(r_k),1} \frac{\partial \bar{u}_1^{(r_k),1}}{\partial x_3} + & \\
 \left. \left(\bar{\sigma}_{21}^{(r_k),1} + \sigma_{11}^{(r_k),0}(t_1) \frac{\partial \bar{u}_2^{(r_k),1}}{\partial x_1} \right) \frac{\partial \bar{u}_2^{(r_k),1}}{\partial x_1} + \right. & \\
 \bar{\sigma}_{22}^{(r_k),1} \frac{\partial \bar{u}_2^{(r_k),1}}{\partial x_2} + \bar{\sigma}_{13}^{(r_k),1} \frac{\partial \bar{u}_1^{(r_k),1}}{\partial x_3} + & \\
 \left. \left(\bar{\sigma}_{31}^{(r_k),1} + \sigma_{11}^{(r_k),0}(t_1) \frac{\partial \bar{u}_3^{(r_k),1}}{\partial x_1} \right) \frac{\partial \bar{u}_3^{(r_k),1}}{\partial x_1} + \bar{\sigma}_{32}^{(r_k),1} \frac{\partial \bar{u}_3^{(r_k),1}}{\partial x_2} + \right. & \\
 \left. \bar{\sigma}_{23}^{(r_k),1} \frac{\partial \bar{u}_2^{(r_k),1}}{\partial x_3} + \bar{\sigma}_{33}^{(r_k),1} \frac{\partial \bar{u}_3^{(r_k),1}}{\partial x_3} \right] dx_1 dx_2 dx_3 \Big] - & \\
 \int_0^{\ell_{30}} \int_{(\ell_1 - \ell_{10})/2}^{(\ell_1 + \ell_{10})/2} \frac{1}{s} \sigma_{11}^{(r_1),0}(t_1) \frac{\partial f^-}{\partial x_1} \bar{u}_1^{(r_1),1} \Big|_{x_2 = h_F^-} dx_1 dx_3 - & \\
 \int_0^{\ell_{30}} \int_{(\ell_1 - \ell_{10})/2}^{(\ell_1 + \ell_{10})/2} \frac{1}{s} \sigma_{11}^{(r_2),0}(t_1) \frac{\partial f^+}{\partial x_1} \bar{u}_1^{(r_2),1} \Big|_{x_2 = h_F^+} dx_1 dx_3 - & \\
 \int_0^{\ell_{30}} \int_{(\ell_1 - \ell_{10})/2}^{(\ell_1 + \ell_{10})/2} \frac{1}{s} \sigma_{11}^{(r_2),0}(t_1) \frac{\partial f^-}{\partial x_1} \bar{u}_1^{(r_2),1} \Big|_{x_2 = (h_F^+ h_C) -} dx_1 dx_3 - & \\
 \int_0^{\ell_{30}} \int_{(\ell_1 - \ell_{10})/2}^{(\ell_1 + \ell_{10})/2} \frac{1}{s} \sigma_{11}^{(r_3),0}(t_1) \frac{\partial f^+}{\partial x_1} \bar{u}_1^{(r_3),1} \Big|_{x_2 = (h_F^+ h_C) +} dx_1 dx_3. & \quad (31)
 \end{aligned}$$

By applying the standard procedure we obtain the equilibrium equation in (27) and all boundary and contact conditions (28) – (30) written for stresses from the relation

$$\delta \Pi = \sum_{k=1}^3 \left[\frac{\partial \Pi}{\partial \bar{u}_1^{(r_k)}} \delta \bar{u}_1^{(r_k)} + \frac{\partial \Pi}{\partial \bar{u}_2^{(r_k)}} \delta \bar{u}_2^{(r_k)} + \frac{\partial \Pi}{\partial \bar{u}_3^{(r_k)}} \delta \bar{u}_3^{(r_k)} \right] = 0 \quad (32)$$

As has been noted above the functional (32) is written for Case 2. By changing the integrating interval $[0, \ell_{30}]$ in the last four integrals in equation (32) with the interval $[0, \ell_3]$ we obtain the corresponding functional for Case 1.

Thus, after establishing the foregoing functional by usual procedure the FEM technique is applied for obtaining the numerical results. In this case the domain $V (= V^{(r_1)} \cup V^{(r_2)} \cup V^{(r_3)})$ is divided into a finite number of finite elements in the form as rectangular prism (brick) elements with eight nodes. The number of finite elements is determined from the convergence requirement of the numerical results. We should note that all computer programmes used in the numerical investigations carried out have been composed by the authors in the package FTN77.

In the paper by Akbarov, Yahnioglu and Rzayev (2007) it is established that under investigation of the buckling delamination around the cracks contained in a plate, the numerical results on the critical parameter attained by the use of the singular type finite elements in the vicinity of the crack tips coincide (with very high accuracy) with those attained by the use of the ordinary type finite elements in the vicinity of the crack tips. According to this statement, in the present investigation the finite elements containing the crack tips (fronts) are also ordinary brick elements. In this way, we simply establish the FEM modeling of the problems under consideration.

Thus, by employing the FEM algorithm detailed above we calculate the values of the Laplace transform of the sought values. The values of the original of the sought functions are determined by the use of the method by Schapery (1966).

5 Numerical Results and Discussion

The material of the face layers is supposed to be linearly viscoelastic with the operators

$$E^{*(2)} = E_0^{(2)} [1 - \omega_0 R_\alpha^* (-\omega_0 - \omega_\infty)],$$

$$v^{*(2)} = v_0^{(2)} \left[1 + \frac{1 - 2v_0^{(2)}}{2v_0^{(2)}} \omega_0 R_\alpha^* (-\omega_0 - \omega_\infty) \right] \quad (33)$$

where $E_0^{(2)}$ and $v_0^{(2)}$ are the instantaneous values of Young's modulus and of Poisson coefficient, respectively; α , ω_0 and ω_∞ are the rheological parameters of the covering layers' materials, R_α^* is the fractional-exponential operator of Rabotnov (1977) and this operator is determined as

$$R_\alpha^* \varphi(t) = \int_0^t R_\alpha(\beta, t - \tau) \varphi(\tau) d\tau \quad (34)$$

where

$$R_\alpha(\beta, t) = t^\alpha \sum_{n=0}^{\infty} \frac{\beta^n t^{n(1+\alpha)}}{\Gamma((1+n)(1+\alpha))}, \quad -1 < \alpha \leq 0. \tag{35}$$

In equation (36), $\Gamma(x)$ is the Gamma function.

The material of the core layer is supposed to be pure elastic with mechanical characteristics $E^{(1)}$ (Young’s modulus) and $\nu^{(1)}$ (Poisson coefficient).

We introduce the dimensionless rheological parameter $\omega = \omega_\infty/\omega_0$ and the dimensionless time $t' = \omega_0^{1/(1+\alpha)}t$. For concrete numerical investigations the suitable initial imperfection modes of the crack edge surfaces can be selected as follows.

For Case 1:

$$f^\pm(x_1) = \pm \ell_{10} \sin^2 \left(\pi \left(x_1 - \frac{\ell_1 - \ell_{10}}{2} \right) / \ell_{10} \right), \tag{36}$$

For Case 2:

$$f^\pm(x_1, x_3) = \pm \ell_{10} \sin^2 \left(\pi \left(x_1 - \frac{\ell_1 - \ell_{10}}{2} \right) / \ell_{10} \right) \sin^2 \left(\frac{\pi}{2\ell_{30}} (\ell_{30} - x_3) \right) \tag{37}$$

Thus, we turn to the analysis of the numerical results and first, we consider pure elastic stability loss buckling delamination which takes place at $t' = 0$ and $t' = \infty$. In these cases the critical values of the averaged strain $\delta = ph/(2E_0^{(2)}h_F + h_C E^{(1)})$ are calculated. The critical values for δ attained at $t' = 0$ and at $t' = \infty$ are denoted through $\delta_{cr,0}$ ($= p_{cr,0}h/(2E_0^{(2)}h_F + h_C E^{(1)})$) and $\delta_{cr,\infty}$ ($= p_{cr,\infty}h/(2E_0^{(2)}h_F + h_C E^{(1)})$) respectively. We consider separately the numerical results obtained in Case 1 and in Case 2 and assume that $h/\ell_1 = 0.15$, $\nu_0^{(1)} = \nu^{(2)} = 0.3$. At the same time, introduce the parameter $\gamma = \ell_3/\ell_1$.

5.1 Numerical results attained in Case 1.

First we analyze the numerical results regarding the pure elastic buckling delamination which takes place at $t' = 0$ and $t' = \infty$. Table 1 shows the values of $\delta_{cr,0}$ calculated for various $E_0^{(2)}/E^{(1)}$, h_F/ℓ_1 and γ under $\ell_{10}/\ell_1 = 0.5$.

According to the well known mechanical consideration, the numerical results attained in the case under consideration must approach the certain asymptote with γ .

This prediction is proven with the data given in Table 1. Moreover, the results obtained in the case under consideration must approach the corresponding results

Table 1: The values of $\delta_{cr,0}$ attained for various h_F/ℓ_1 , $E_0^{(2)}/E^{(1)}$ and γ under (Case 1).

γ	h_F/ℓ_1											
	0.0250				0.0375				0.0500			
	$E_0^{(2)}/E^{(1)}$											
	1	5	10	1	5	10	1	5	10	1	5	10
1	0.0120	0.0263	0.0432	0.0217	0.0601	0.1044	0.0336	0.1131	0.2045			
2	0.0111	0.0241	0.0394	0.0198	0.0542	0.0934	0.0304	0.1009	0.1812			
3	0.0109	0.0238	0.0387	0.0195	0.0532	0.0915	0.0298	0.0989	0.1772			
4	0.0109	0.0236	0.0385	0.0193	0.0528	0.0909	0.0296	0.0981	0.1759			
5	0.0108	0.0235	0.0384	0.0193	0.0526	0.0906	0.0295	0.0978	0.1752			
6	0.0108	0.0235	0.0383	0.0193	0.0526	0.0904	0.0295	0.0977	0.1749			
8	0.0108	0.0235	0.0382	0.0192	0.0525	0.0903	0.0294	0.0975	0.1745			

Table 2: The values of $\delta_{cr,0}$ (present work Rzayev(2002)) attained under $\ell_{10}/\ell_1 = 0.5$, $h/\ell_1 = 0.15$ and $\gamma = 8$ for various values of h_F/ℓ_1 and $E_0^{(2)}/E^{(1)}$ (Case 1).

h_F/ℓ_1	$E_0^{(2)}/E^{(1)}$			
	1	5	10	20
0.0250	0.0108	0.0235	0.0382	0.0656
	0.0081	0.0269	0.0456	0.0722
0.0375	0.0192	0.0525	0.0903	0.1581
	0.0165	0.0471	0.0796	0.1304

attained in a paper by Rzayev (2002) with γ , because in the mentioned paper the plane-strain state (i.e. the case $\gamma = \infty$) is considered.

Table 2 shows simultaneously the values of $\delta_{cr,0}$ obtained in the present investigation (upper number) under $\gamma = 8$ and the results attained in the paper by Rzayev (2002) (lower number). The comparison shows that the results attained in the present investigation agree quite well with the corresponding results obtained by Rzayev (2002). This statement validates also the reliability of the algorithm and packed programmes used in the present investigation.

These packed programmes have been composed by the authors. Moreover, it follows from Tables 1 and 2 that the values of $\delta_{cr,0}$ decrease with γ , but increase with $E_0^{(2)}/E^{(1)}$ and h_F/ℓ_1 . A more detailed illustration of the influence of the parameters $E_0^{(2)}/E^{(1)}$ and h_F/ℓ_1 on the values of the $\delta_{cr,0}$ (upper number) and $\delta_{cr,\infty}$ (lower number) is given in Tables 3 and 4 in the case where $\ell_{10}/\ell_1 = 0.5$. Note that under calculation of the values of the $\delta_{cr,\infty}$ it is assumed that $\omega = 2$.

Fig 2 shows the graphs of the dependencies among $\delta_{cr,0}$, $\delta_{cr,\infty}$ and ℓ_{10}/ℓ_1 . Note that these graphs are constructed for various $E_0^{(2)}/E^{(1)}$ under $\gamma = 1$, $\omega = 2$. It follows from Fig. 2 that, as it can be predicted, the values of $\delta_{cr,0}$ and $\delta_{cr,\infty}$ increase monotonically with a decrease in the values of ℓ_{10}/ℓ_1 . Fig. 3 shows schematically the distribution of $u_2^{(2)} E_0^{(2)}/(\ell_1 p)$ with respect to $x (= x_1)$ and $z (= \ell_3 - x_3)$ under $x_2 = h_F - 0$, $\ell_3/2 \leq x_3 \leq \ell_3$, $0 \leq x_1 \leq \ell_1/2$, in other words Fig. 3 shows the buckling mode of the crack's lower edge for the compressive force which is very near the critical force, i.e. for the values of the parameter δ for which the relation $|\delta - \delta_{cr,0}| < 10^{-3}$ is satisfied. Under construction of this buckling mode the problem symmetry with respect to $x_1 = \ell_1/2$ and $x_3 = \ell_3/2$ is taken into account and it is assumed $\gamma = 1$, $h_F/\ell_1 = 0.0375$, $\ell_{10}/\ell_1 = 0.5$ and $E_0^{(2)}/E^{(1)} = 10$. It should

Table 3: The values of $\delta_{cr,0}$ (upper number) and $\delta_{cr,\infty}$ (lower number) obtained under $\gamma = 1$, $\ell_{10}/\ell_1 = 0.5$ and $h_F/\ell_1 = 0.0375$ for various values of $E_0^{(2)}/E^{(1)}$ (Case 1).

$E_0^{(2)}/E^{(1)}$	$\delta_{cr,0}/\delta_{cr,\infty}$
0.3	<u>0.0145</u> 0.0101
0.5	<u>0.0166</u> 0.0115
1	<u>0.0217</u> 0.0153
2	<u>0.0317</u> 0.0224
5	<u>0.0601</u> 0.0429
10	<u>0.1044</u> 0.0749
20	<u>0.1845</u> 0.1342

be noted that, the buckling delamination mode constructed for other values of the problem parameters remain similar to that shown in given in Fig. 3

Now we assume that the material of the face layers of the sandwich plate is viscoelastic with the rheological parameters $\alpha = -0.5$ and $\omega = 2.0$. Consider the numerical results attained for the critical time t'_{cr} . These results are given in Table 5 for various $E_0^{(2)}/E^{(1)}$, h_F/ℓ_1 and δ for the case where $\gamma = 1.0$ and $\ell_{10}/\ell_1 = 0.5$.

Note that the external compressive force, i.e. the values of the parameter δ must satisfy the following relation so that the viscoelastic buckling delamination of the plate considered will occur.

Therefore, under obtaining the results illustrated in Table 5 the values of δ are selected according to the relation (38). It follows from Table 5 that the values of t'_{cr} decrease with an increase in the values of δ .

Table 6 shows the influence of the rheological parameters ω and α on the values of t'_{cr} for various values of $E_0^{(2)}/E^{(1)}$ in the case where $\delta = 0.036$, $\gamma = 1$, $h_F/\ell_1 = 0.0250$ and $\ell_{10}/\ell_1 = 0.5$. It follows from Table 6 that the values of t'_{cr} increase with ω and with a decrease in the absolute values of the parameter α . Note that this result occurs (in the quantitative sense) for the other values of the problem parameters δ , γ and h_F/ℓ_1 . Moreover, note that this result agrees with the known

Table 4: The values of $\delta_{cr,0}$ (upper number) and $\delta_{cr,\infty}$ (lower number) obtained under $\gamma = 1$ and $\ell_{10}/\ell_1 = 0.5$ for various values of $E_0^{(2)}/E^{(1)}$ and h_F/ℓ_1 (Case 1).

h_F/ℓ_1	$E_0^{(2)}/E^{(1)}$			
	1	2	5	10
0.01250	<u>0.0055</u>	<u>0.0063</u>	<u>0.0088</u>	<u>0.0128</u>
	0.0038	0.0043	0.0061	0.0090
0.01875	<u>0.0083</u>	<u>0.0101</u>	<u>0.0158</u>	<u>0.0247</u>
	0.0058	0.0071	0.0110	0.0174
0.02500	<u>0.0120</u>	<u>0.0157</u>	<u>0.0263</u>	<u>0.0432</u>
	0.0084	0.0110	0.0186	0.0308
0.03125	<u>0.0166</u>	<u>0.0228</u>	<u>0.0410</u>	<u>0.0694</u>
	0.0116	0.0161	0.0291	0.0497
0.03750	<u>0.0217</u>	<u>0.0317</u>	<u>0.0601</u>	<u>0.1044</u>
	0.0153	0.0224	0.0429	0.0749
0.04375	<u>0.0275</u>	<u>0.0421</u>	<u>0.0841</u>	<u>0.1490</u>
	0.0193	0.0298	0.0599	0.1070
0.05000	<u>0.0336</u>	<u>0.0543</u>	<u>0.1131</u>	<u>0.2045</u>
	0.0236	0.0384	0.0805	0.1465
0.05625	<u>0.0400</u>	<u>0.0679</u>	<u>0.1477</u>	<u>0.2725</u>
	0.0281	0.0479	0.1048	0.1946

mechanical consideration, so that the viscoelastic material of the face layers of the plate becomes more stiff one with ω , but an increase in the absolute values of the parameter α corresponds to the decreasing of the stiff of the face layer's material.

5.2 Numerical results attained in Case 2

Within the foregoing assumptions and notation we analyze the numerical results obtained in Case 2. As in the previous case, first we consider the pure elastic buckling delamination of the rectangular sandwich plate containing a rectangular surface edge-crack the edge surfaces of which have the initial imperfection described by the equation (37). Note that in Case 2 the crack geometry is characterized not only by the initial imperfection mode and the parameters h_F/ℓ_1 and ℓ_{10}/ℓ_1 but also with the parameter ℓ_{30}/ℓ_1 through which the crack depth along the Ox_3 axis is estimated.

Thus we consider the results given in Table 7 which shows the values of $\delta_{cr,0}$ (upper number) and $\delta_{cr,\infty}$ (lower number) for various $E_0^{(2)}/E^{(1)}$ under $\gamma = 1$, $\ell_{10}/\ell_1 = 0.5$, $\ell_{30}/\ell_1 = 0.3$ and $h_F/\ell_1 = 0.0375$. Moreover, for the same values of the parameters γ , ℓ_{10}/ℓ_1 and ℓ_{30}/ℓ_1 Table 8 shows the influence of the thickness of the face layer,

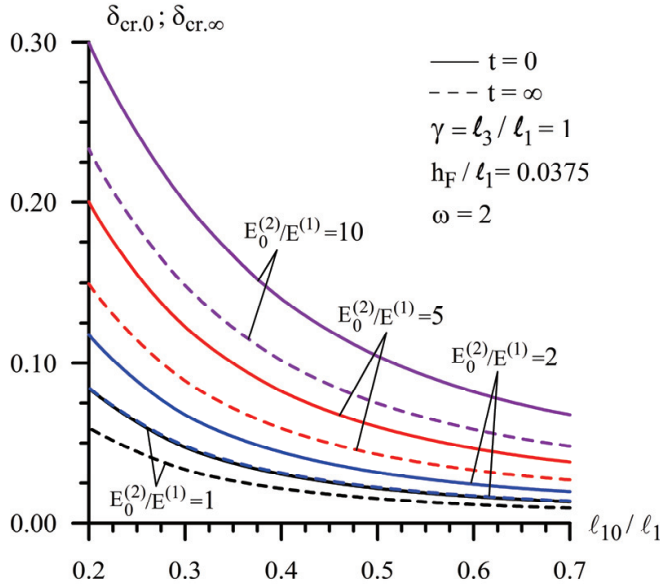


Figure 2: The graphs of the dependence among $\delta_{cr,0}$, $\delta_{cr,\infty}$ and ℓ_{10}/ℓ_1 constructed for various values of $E_0^{(2)}/E^{(1)}$ (Case 1).

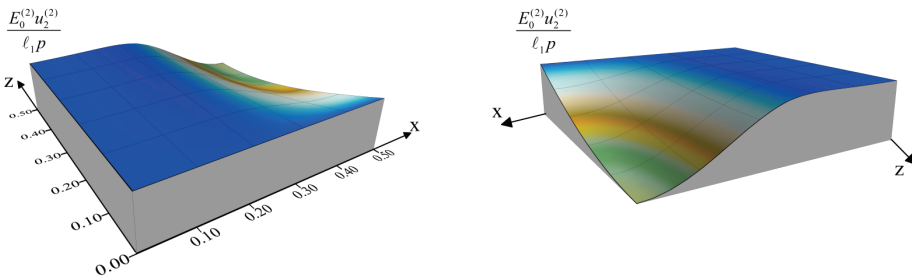


Figure 3: The buckling delamination mode for the case where $h_F/\ell_1 = 0.0375$, $\ell_{10}/\ell_1 = 0.5$, $E_0^{(2)}/E^{(1)} = 10$ (Case 1).

i.e. of the values of h_F/ℓ_1 on the values of $\delta_{cr,0}$ (upper number) and $\delta_{cr,\infty}$ (lower number) for various $E_0^{(2)}/E^{(1)}$.

The comparison of the results given Table 7 and 8 with the corresponding results given in Tables 3 and 4 respectively show that for the concrete selected values of the problem parameters. The values of $\delta_{cr,0}$ and $\delta_{cr,\infty}$ obtained in Case 2 are grater

Table 5: The values of t_{cr} obtained under $\gamma = 1$, $\ell_{10}/\ell_1 = 0.5$, $\omega = 2$ and $\alpha = -0.5$ for various values of $E_0^{(2)}/E^{(1)}$, h_F/ℓ_1 and δ (Case 1).

$E_0^{(2)}/E^{(1)}$	h_F/ℓ_1					
	0.0375		0.0250		0.0125	
	δ	t_{cr}	δ	t_{cr}	δ	t_{cr}
1	0.0210	0.001	0.0110	0.010	0.0052	0.003
	0.0200	0.008	0.0100	0.104	0.0050	0.010
	0.0190	0.034	0.0900	1.885	0.0048	0.029
2	0.0300	0.003	0.0146	0.005	0.0058	0.007
	0.0292	0.008	0.0140	0.020	0.0052	0.093
	0.0285	0.017	0.0133	0.066	0.0046	2.261
5	0.0576	0.001	0.0238	0.015	0.0083	0.003
	0.0570	0.003	0.0233	0.025	0.0079	0.011
	0.0564	0.004	0.0228	0.041	0.0076	0.033
10	0.0990	0.003	0.0400	0.007	0.0120	0.004
	0.0935	0.021	0.0360	0.113	0.0115	0.016
	0.0880	0.096	0.0320	5.171	0.0110	0.048

than corresponding ones obtained in Case 1. Moreover, it follows from the results given in Tables 7 and 8 that in Case 2, as in Case 1, the values of $\delta_{cr,0}$ and $\delta_{cr,\infty}$ increase monotonically with $E_0^{(2)}/E^{(1)}$ and h_F/ℓ_1 .

Fig. 4 shows the graphs of the dependence among $\delta_{cr,0}$, $\delta_{cr,\infty}$ and ℓ_{10}/ℓ_1 for various $E_0^{(2)}/E^{(1)}$ under $\gamma = 1$, $h_F/\ell_1 = 0.0375$, $\ell_{30}/\ell_1 = 0.3$ and $\omega = 2.0$. It follows from these results that the values of the critical strains decrease with the length of the edge crack in the direction of the Ox_1 axis. Although this conclusion is illustrated for the selected values of the problem parameters h_F/ℓ_1 and ℓ_{30}/ℓ_1 , but that holds also for the other possible values of these parameters.

Consider the influence of the depth of the edge-crack in the direction of the Ox_3 axis on the values of the $\delta_{cr,0}$ and $\delta_{cr,\infty}$. Fig. 5 illustrates this influence for various value of $E_0^{(2)}/E^{(1)}$ in the case where $\ell_{10}/\ell_1 = 0.5$, $h_F/\ell_1 = 0.0375$ and $\gamma = 1$. Note that in these figures the values $\delta_{cr,0}$ and $\delta_{cr,\infty}$ attained $\bullet \bullet$ for the band crack are also indicated. According to the mechanical consideration, there must exist such values of ℓ_{30}/ℓ_1 (denoted by $(\ell_{30}/\ell_1)^*$) before (after) which, i.e. in the cases where $\ell_{30}/\ell_1 < (\ell_{30}/\ell_1)^*$ ($\ell_{30}/\ell_1 > (\ell_{30}/\ell_1)^*$) the values of $\delta_{cr,0}$ and $\delta_{cr,\infty}$ attained in Case 2 are greater (less) than the corresponding values of those attained in Case 1. Because, according to the problem formulation, in Case 1 the plate ends at $x_3 = 0$ and $x_3 = \ell_3$ are simply supported; but in Case 2 the plate end at $x_3 = \ell_3$ is simply

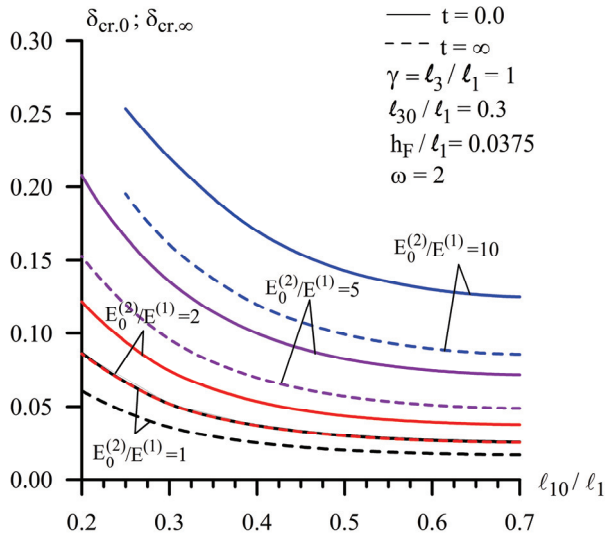


Figure 4: The graphs of the dependence among $\delta_{cr,0}$, $\delta_{cr,\infty}$ and ℓ_{10}/ℓ_1 constructed for various values of $E_0^{(2)}/E^{(1)}$ (Case 2).

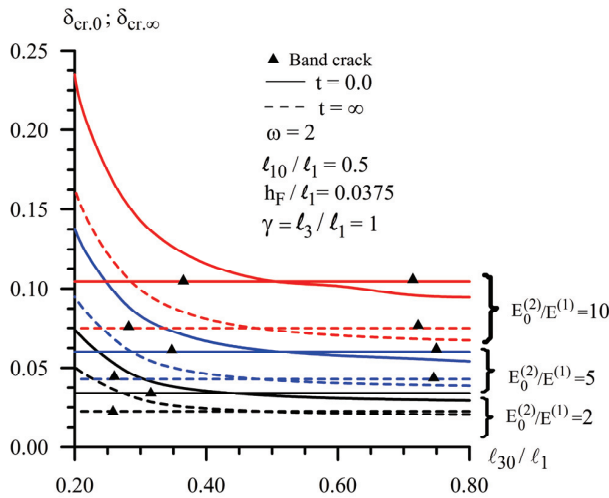


Figure 5: The buckling delamination mode for the case where $h_F/\ell_1 = 0.0375$, $\ell_{10}/\ell_1 = 0.5$, $E_0^{(2)}/E^{(1)} = 10$ (Case 2).

Table 6: The values of t_{cr} obtained under $\gamma = 1, \ell_{10}/\ell_1 = 0.5, h_F/\ell_1 = 0.0250$ and $\delta = 0.0360$ for various values of ω and α (Case 1).

$E_0^{(2)}/E^{(1)}$	δ	ω	α	t_{cr}
2	0.0140	1		0.014
		2	-0.5	0.020
		3		0.032
		2	-0.3	0.051
			-0.5	0.020
			-0.7	0.002
5	0.0233	1		0.016
		2	-0.5	0.025
		3		0.042
		2	-0.3	0.059
			-0.5	0.025
			-0.7	0.003
10	0.0360	1		0.052
		2	-0.5	0.113
		3		0.414
		2	-0.3	0.173
			-0.5	0.113
			-0.7	0.042

supported, but the plate end at $x_3 = 0$ is free.

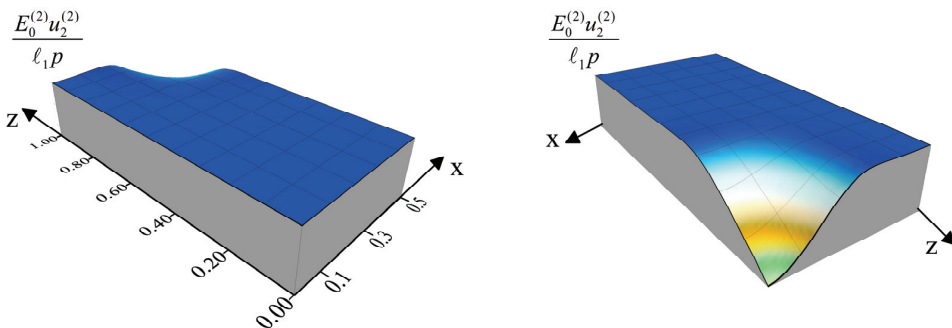


Figure 6: The buckling delamination mode obtained for the case where $\ell_{30}/\ell_1 = 0.3, E_0^{(2)}/E^{(1)} = 10$ (Case 2).

Now we handle the question of how the buckling delamination mode depends on

Table 7: The values of $\delta_{cr,0}$ (upper number) and $\delta_{cr,\infty}$ (lower number) obtained under $\gamma = 1$, $\ell_{10}/\ell_1 = 0.5$, $\ell_{30}/\ell_1 = 0.3$ and $h_F/\ell_1 = 0.0375$ for various values of $E_0^{(2)}/E^{(1)}$ (Case 2).

$E_0^{(2)}/E^{(1)}$	$\delta_{cr,0}/\delta_{cr,\infty}$
0.3	<u>0.0199</u>
	0.0134
0.5	<u>0.0229</u>
	0.0154
1	<u>0.0300</u>
	0.0204
2	<u>0.0437</u>
	0.0299
5	<u>0.0827</u>
	0.0570
10	<u>0.1428</u>
	0.0992
20	<u>0.2496</u>
	0.1768

the crack depth, i.e. on the parameter ℓ_{30}/ℓ_1 . Fig. 6 shows schematically the distribution of $u_2^{(2)}E_0^{(2)}/(\ell_1 p)$ with respect to $x (= x_1)$ and $z (= \ell_3 - x_3)$ under $x_2 = h_F - 0$, in other words Fig. 6 shows the buckling mode corresponding to the compressive force which is very near the critical force, i.e. for the values of the parameter δ for which the relation $|\delta - \delta_{cr,0}| < 10^{-3}$ is satisfied. Although the illustrated distributions are constructed for the case where $E_0^{(2)}/E^{(1)} = 10$, $h_F/\ell_1 = 0.0375$, $\gamma = 1$ and $\ell_{30}/\ell_1 = 0.3$ (Fig. 6), they hold (in a qualitative sense) in the cases where $\ell_{30}/\ell_1 > 0.3$ for the selected values of the problem parameters $E_0^{(2)}/E^{(1)}$ and h_F/ℓ_1 . But, in the cases where $\ell_{30}/\ell_1 < \chi < 0.6$ is satisfied the buckling of the edge crack's surface has a complicated mode. Note that the values of the χ depend on the problem parameters h_F/ℓ_1 , ℓ_{10}/ℓ_1 and $E_0^{(2)}/E^{(1)}$. As an example, we consider the distribution of $u_2^{(2)}E_0^{(2)}/(\ell_1 p)$ with respect to $x (= x_1)$ and $z (= x_3)$ for the same values of the problem parameters under $\ell_{30}/\ell_1 = 0.2$, i.e. under $\ell_{30}/\ell_{10} = 0.5$. Fig. 7 shows the graphs of this distribution for the cases where $\delta = 0.165$ (Fig. 7a), 0.2145 (Fig. 7b), 0.2150 (Fig. 7c) and 0.2151 (Fig. 7d). Consequently, Fig. 7 shows simultaneously the evolution of the initial imperfection mode before the buckling mode. Analyses of the results given in Figs. 6 and 7, and other results which are not given here show that the buckling mode of the edge rectangular crack

Table 8: The values of $\delta_{cr,0}$ (upper number) and $\delta_{cr,\infty}$ (lower number) attained under $\gamma = 1$, $\ell_{10}/\ell_1 = 0.5$ and $\ell_{30}/\ell_1 = 0.3$ for various values of $E_0^{(2)}/E^{(1)}$ and h_F/ℓ_1 (Case 2).

h_F/ℓ_1	$E_0^{(2)}/E^{(1)}$			
	1	2	5	10
0.01250	0.0083	0.0095	0.0133	0.0194
	0.0055	0.0064	0.0089	0.0131
0.01875	0.0121	0.0148	0.0230	0.0358
	0.0081	0.0100	0.0156	0.0245
0.02500	0.0171	0.0224	0.0374	0.0611
	0.0116	0.0152	0.0256	0.0422
0.03125	0.0232	0.0320	0.0572	0.0964
	0.0157	0.0218	0.0393	0.0668
0.03750	0.0300	0.0437	0.0827	0.1428
	0.0204	0.0299	0.0570	0.0992
0.04375	0.0375	0.0575	0.1142	0.2015
	0.0255	0.0393	0.0788	0.1400
0.05000	0.0454	0.0733	0.1523	0.2739
	0.0309	0.0500	0.1047	0.1899
0.05625	0.0536	0.0910	0.1973	0.3623
	0.0364	0.0620	0.1352	0.2500

depends significantly on the values of the ratio ℓ_{30}/ℓ_{10} . So that, there exists such a value of the ratio $\ell_{30}/\ell_{10} = \chi$ after which, i.e. for the case where $(\ell_{30}/\ell_{10}) > \chi$ the buckling mode is similar to the initial imperfection mode, but in the cases where $(\ell_{30}/\ell_{10}) < \chi$ the buckling mode has a complicated character, such as shown in Fig. 7. As noted above, the values of χ depend on the values of the problem parameters, especially, on the values of h_F/ℓ_1 . The graphs given in Fig. 8 illustrate schematically this dependence in the cases where $E_0^{(2)}/E^{(1)} = 10$ under $\ell_{30}/\ell_1 = 0.2$ and $\ell_{10}/\ell_1 = 0.3$. In Fig.8 the vertical axis shows the values of

$$v = 2u_2^{(2)} \left(\left| \max_{0 \leq x_1/\ell_1 \leq 0.5} u_2^{(2)} - \min_{0 \leq x_1/\ell_1 \leq 0.5} u_2^{(2)} \right| \right)^{-1} \text{ at } x_2 = h_F - 0, x_3 = 0.$$

It follows from the results given in Fig. 8 that the appearance of the complicated buckling delamination modes becomes more suitable with decreasing of the parameter h_F/ℓ_1 . Moreover, Fig. 9 shows the graphs of the dependence between v and x_1/ℓ_1 for various values of ℓ_{30}/ℓ_{10} under

$$E_0^{(2)}/E^{(1)} = 10, \quad h_F/\ell_1 = 0.0375, \quad \ell_{30}/\ell_1 = 0.2.$$

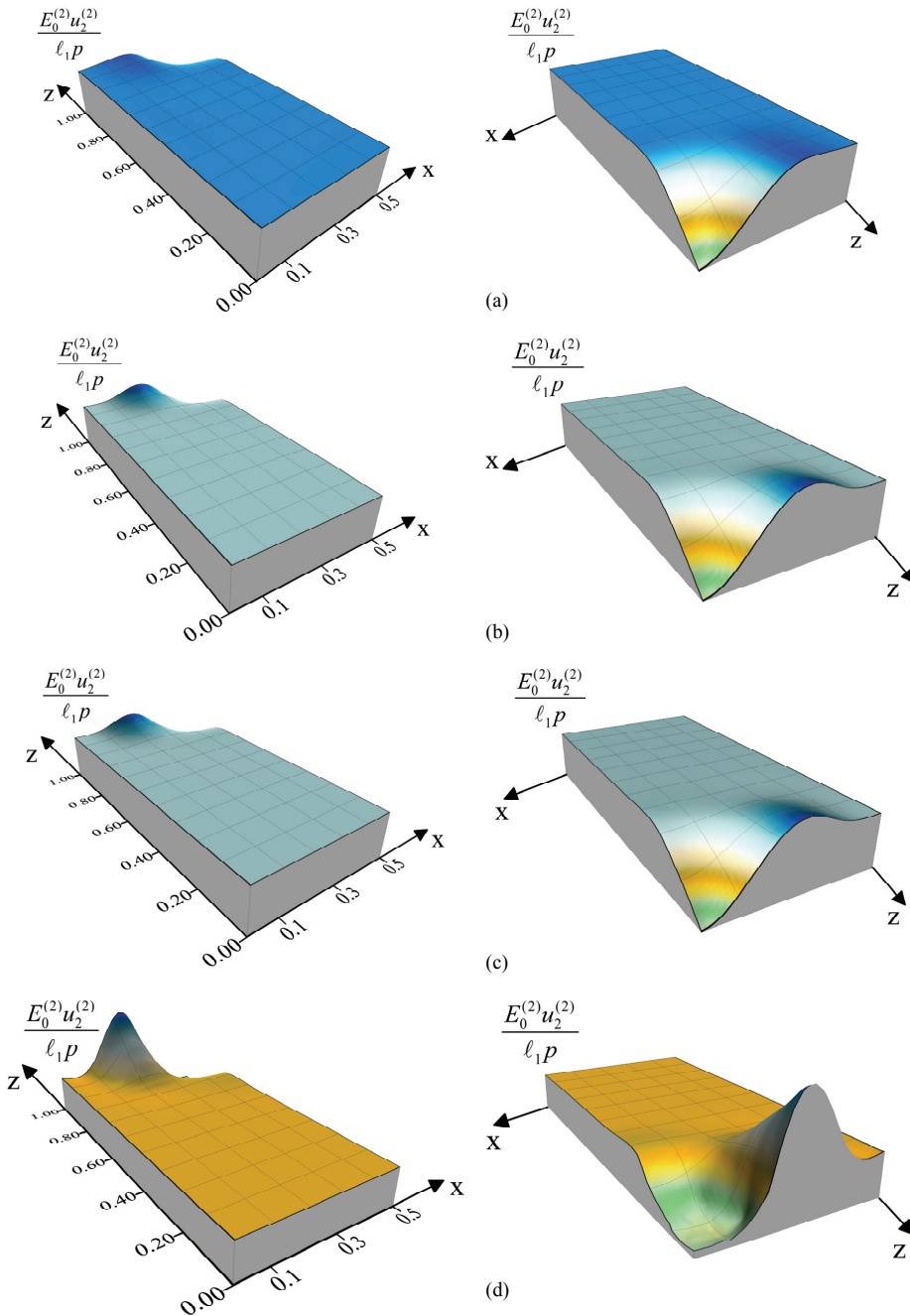


Figure 7: The evolution of the buckling delamination mode with δ : a) $\delta = 0.1650$, b) $\delta = 0.2145$, c) $\delta = 0.2150$, d) $\delta = 0.2151$ under $\ell_{30}/\ell_1 = 0.2$, $E_0^{(2)}/E^{(1)} = 10$

It follows from these graphs that, for the considered values of the problem parameters in the case where $\ell_{30}/\ell_{10} = 0.7272$ the buckling delamination mode is similar to the initial imperfection mode. But for the cases where $(\ell_{30}/\ell_{10}) < \chi = 0.7272$ the buckling delamination mode becomes complicated in the sense shown in Figs. 7, 8 and 9. It follows from these results that the complicated buckling modes observed in the experimental investigations carried out by Evans and Hutchinson (1995), Gioia and Ortiz (1997), Hutchinson and Suo (1992), Hutchinson et al. (1992), Nilson and Giannakopoulos (1995), Thouless et al. (1994), Wang and Evans (1998) and Moon et. al. (2002) can be described within the scope of the approach proposed and developed in the present paper.

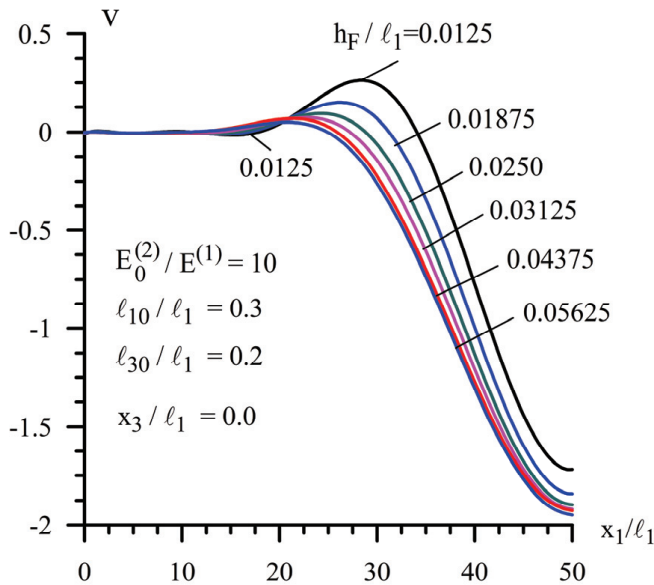


Figure 8: The influence of the h_F/ℓ_1 on the distribution of the vertical displacement of the crack's edge at $x_3 = 0$ with respect to x_1/ℓ_1 .

The violation of the initial imperfection mode of the crack's edges under its evolution with external compressive forces can be explained as follows. In the case considered, the investigation on the evolution of the crack edge-surfaces can be considered approximately as the investigation of the buckling of "rectangular plate", whose edges are supported elastically. Namely, the "rectangular plate" mentioned above is formed from the part of the plate occupying the region consisting of the part of the face layer which is between the crack's edge surface and free face of this

layer. During the evolution of the initial imperfection in the ends of this “rectangular plate” various types of stresses and displacements arise. These distributions depend significantly on the ratios ℓ_{30}/ℓ_{10} , h_F/ℓ_1 and determine the buckling mode. Moreover, for the clarity of the foregoing discussion the following known fact in the theory of stability of the rectangular plates should be remembered.

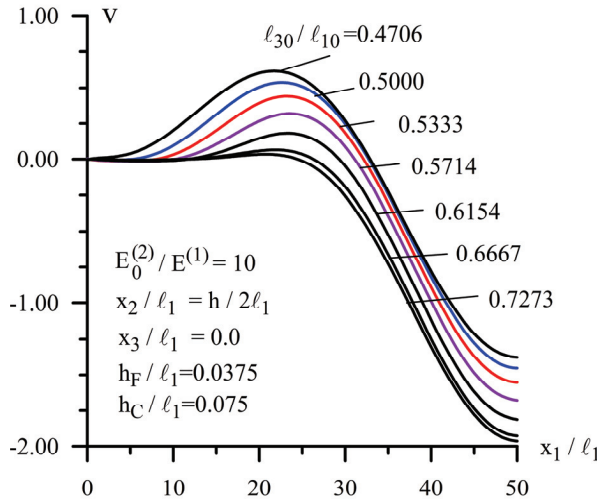


Figure 9: The influence of the ℓ_{30}/ℓ_{10} on the distribution of the vertical displacement of the crack’s edge at $x_3 = 0$ with respect to x_1/ℓ_1 .

Suppose that the stability loss of the rectangular plate without any initial imperfection with the length of ℓ_{10} and the width ℓ_{30} is considered within the scope of the Euler (bifurcation) approach. Furthermore, assume that at the ends of this plate act the normal and tangential forces. As it follows from the corresponding theoretical and experimental investigations (see, for example, a monograph by Volmir (1967)), in such cases the stability loss modes of the rectangular plates depend on the ratio of the length to the width of that.

The large number of numerical results which are not given here show that under the buckling delamination the displacement $u_2^{(1)}$ at $x_2 = h_F + 0$, for $-\ell_{10}/2 < x_1 < \ell_{10}/2$, $0 < x_3 < \ell_{30}$, i.e. the vertical displacement of the upper edge surface of the edge crack is significantly less and can be neglected with respect to that considered above, i.e. with respect to the vertical displacement of the lower edge surface of this crack. Therefore, in the cases where $(\ell_{30}/\ell_{10}) < \chi$, i.e. in the cases where the complicated buckling delamination modes appear, the contact of the crack’s edges may arise in the certain stage of the evolution of the initial imperfection of

these edges. It should be noted that this statement is not taken into account in the present investigation. Nevertheless, the results discussed above and relating the cases where $(\ell_{30}/\ell_{10}) < \chi$ give the important information on the evolution stages of the interface crack's edges.

Now, we consider the numerical results attained for the critical time, i.e. for the t'_{cr} . As in Case 1, under obtaining these results we assume that the values of the strain caused by the external compressive force satisfy the inequality-relation (38).

Table 9: The values of t_{cr} attained under $\gamma = 1, \ell_{10}/\ell_1 = 0.5, \ell_{30}/\ell_1 = 0.3, \omega = 2$ and $\alpha = -0.5$ for various values of $E_0^{(2)}/E^{(1)}, h_F/\ell_1$ and δ (Case 2).

$E_0^{(2)}/E^{(1)}$	h_F/ℓ_1					
	0.0375		0.0250		0.0125	
	δ	t_{cr}	δ	t_{cr}	δ	t_{cr}
1	0.0280	0.004	0.0160	0.004	0.0080	0.001
	0.0270	0.012	0.0150	0.023	0.0070	0.046
	0.0260	0.029	0.0140	0.100	0.0060	1.591
2	0.0420	0.001	0.0206	0.005	0.0087	0.007
	0.0412	0.002	0.0200	0.014	0.0081	0.036
	0.0405	0.005	0.0193	0.030	0.0075	0.163
5	0.0780	0.002	0.0340	0.009	0.0126	0.001
	0.0720	0.029	0.0336	0.013	0.0123	0.004
	0.0660	0.197	0.0331	0.018	0.0119	0.010
10	0.1375	0.001	0.0560	0.007	0.0175	0.010
	0.1320	0.006	0.0520	0.049	0.0162	0.055
	0.1265	0.020	0.0480	0.293	0.0150	0.302

Table 9 shows the values of t'_{cr} attained for various $h_F/\ell_1, \delta$ and $E_0^{(2)}/E^{(1)}$ under $\omega = 2, \alpha = -0.5, \gamma = 1, \ell_{10}/\ell_1 = 0.5$ and $\ell_{30}/\ell_1 = 0.3$. In the quantitative sense these results agree with the corresponding results obtained in Case 1. The results given in Table 10 illustrate the influence of the rheological parameter ω and α on the values of t'_{cr} . It follows from these results that the values of t'_{cr} increase (decrease) with ω (with absolute values of α).

6 Conclusion

In the present paper the approach was developed and employed for the study of the buckling delamination of the elastic and viscoelastic sandwich rectangular plates containing interface rectangular cracks. The investigation was made within the

Table 10: The values of t_{cr} obtained under $\gamma = 1$, $\ell_{10}/\ell_1 = 0.5$, $\ell_{30}/\ell_1 = 0.3$ and $h_F/\ell_1 = 0.0250$ for various values of ω , α and $E_0^{(2)}/E^{(1)}$ (Case 2).

$E_0^{(2)}/E^{(1)}$	δ	ω	α	t_{cr}
2	0.0200	1		0.010
		2	-0.5	0.014
		3		0.020
		2	-0.3	0.038
			-0.5	0.014
			-0.7	0.001
5	0.0354	1		0.009
		2	-0.5	0.013
		3		0.018
		2	-0.3	0.037
			-0.5	0.013
			-0.7	0.001
10	0.0520	1		0.028
		2	-0.5	0.049
		3		0.105
		2	-0.3	0.096
			-0.5	0.049
			-0.7	0.010

scope of the piecewise homogeneous body model. It was assumed that the edge surfaces of the cracks have initial infinitesimal imperfections and the proposed approach was based on the study of the evolution of this initial imperfections with external compressive forces (with duration of time) for pure elastic (viscoelastic) one. The noted evolution was determined within the scope of the exact 3D geometrically nonlinear field equations of the theory of elasticity and viscoelasticity. For the solution to the corresponding boundary-value problems, the boundary form perturbation techniques, Laplace transform and 3D FEM were employed. The initial imperfection criterion was used as a delamination buckling (stability loss) criterion. For the concrete numerical investigations, two cases were selected. In Case 1 (Case 2) it was assumed that the interface cracks contained by the sandwich plate are rectangular band-cracks (rectangular edge-cracks). The numerical results on the influence of the problem parameter on the values of the critical strain and critical time as well as on the buckling delamination mode were presented and analyzed. According to these analyses, the following main conclusions can be drawn:

- In Case 1 the mode of buckling delamination around the interface rectangular band-cracks is similar to the initial imperfection mode of these cracks which is symmetric with respect to the interface plane;
- In Case 2, the mode of buckling delamination around the interface rectangular edge-cracks depends on the thickness of the face layers of the plate and on values of the ratio ℓ_{30}/ℓ_{10} , where $\ell_{30}(\ell_{10})$ is a depth (length) of the crack;
- The values of the critical strain as well as the values of the critical time decrease with the length and width of the cracks;
- There exists a length of the edge cracks after which the critical values of the strain attained in Case 2 become less than corresponding ones attained in Case 1;
- With the length of the rectangular band-crack along the Ox_3 axis the results attained for the critical strains approach the results attained in the paper by Rzayev (2002);
- The values of the critical strain and time increase with the stiffness of the material of the face layers;
- The numerical results attained and analyzed in the present paper can be taken as standard ones for the estimation of the accuracy (in the qualitative and quantitative senses) of the corresponding numerical results attained within the scope of the approximate plate and bar theories;
- The developed approach gives possibility for mathematical modeling and describing the complicated buckling delamination modes of the stratified layers observed in the corresponding experimental studies.

Acknowledgement: This work was supported by Yildiz Technical University Research Fund. Project number: 2010-05-01-DOP01.

References

- Akbarov, S. D.** (1998): On the three dimensional stability loss problems of elements of constructions fabricated from the viscoelastic composite materials. *Mech. Comp. Mater.*, vol. 34(6), pp. 537-544.
- Akbarov, S. D.** (2007): Three-dimensional in stability problems for viscoelastic composite materials and structural members. *Inter. Appl. Mech.* 43(10),1069-1089.

- Akbarov, S.D., Guz, A.N.** (2000): *Mechanics of Curved Composites*. Kluwer Academic Publishers, Dordrecht/Boston/London.
- Akbarov, S. D., Rzayev, O. G.** (2002a): On the buckling of the elastic and viscoelastic composite circular thick plate with a penny-shaped crack. *Eur. J. Mech. A-Solid*, vol. 21(2), pp. 269-279.
- Akbarov, S. D., Rzayev, O. G.** (2002b): Delamination of unidirectional viscoelastic composite materials. *Mech. Comp. Mater.*, vol. 38(1), pp. 17-24.
- Akbarov, S. D., Rzayev, O. G.** (2003): On the delamination of a viscoelastic composite circular plate. *Inter. Appl. Mech.*, vol. 39(3), pp. 368-374.
- Akbarov, S. D., Sisman, T., Yahnioglu, N.** (1997): On the fracture of the unidirectional composites in compression. *Int. J. Eng. Sci.*, vol. 35(12/13), pp. 1115-1136.
- Akbarov, S. D., Yahnioglu, N.** (2001): The method for investigation of the general theory of stability problems of structural elements fabricated from the viscoelastic composite materials. *Compos. Part B-Eng.*, vol. 32(5), pp. 475-482.
- Akbarov, S. D., Yahnioglu, N., Rzayev, O. G.** (2007): On influence of the singular type finite elements to the critical force in studying the buckling of a circular plate with a crack. *Inter. Appl. Mech.*, Vol. 43(9), pp. 120-129.
- Alaimo, A., Milazzo, A., Orlando, C.** (2008): Global/Local FEM-BEM stress analysis of damaged aircraft structures, *CMES: Computer Modeling in Engineering and Sciences*, vol. 36(1), pp. 23-42.
- Arman, Y., Zor, M., Aksoy, S.** (2006): Determination of critical delamination diameter of laminated composite plates under buckling loads. *Compos. Sci. and Technol.*, vol. 66, pp. 2945-2953.
- Atluri, S. N.** (2005): *Methods of Computer Modeling in Engineering & the Sciences* (Hardcover), Tech. Science. Pres.
- Attaporn, W., H. Koguchi, H.** (2009): Intensity of stress singularity at a vertex and along the free edges of the interface in 3D-dissimilar material joints using 3D-enriched FEM. *CMES: Computer Modeling in Engineering and Sciences*, vol. 39(3), pp. 237-262.
- Bogdanov, V. L., Guz, A. N., Nazarenko, V. M.** (2009): Fracture of a body with a periodic set of coaxial cracks under forced directed along them: an axisymmetric problem. *Inter. Appl. Mech.*, vol. 45(2), pp. 111-124.
- Chai, H., Babcock, C. D., Knauss, W. G.** (1981): One-dimensional modeling of failure in laminated plates by delamination buckling. *Int. J. Solids Struct.*, vol. 17, pp. 1069-1083.
- Evans, A.G. and Hutchinson, J.W.** (1995): The thermo mechanical integrity of thin films and multilayers. *Acta Metal. Mater.*, vol. 43, pp. 2507-2530.

- Gioia, F. and Ortiz, M.** (1997): Delamination of compressed thin films. *Adv. Appl. Mech.*, vol. 33, pp. 120-192.
- Guz, A. N.** (1999): *Fundamentals of The Three-Dimensional Theory of Stability of Deformable Bodies*. Springer-Verlag, Berlin Heidelberg.
- Guz, A. N.** (2008a): *Fundamentals of The Compressive Fracture Mechanics of Composites: Fracture in Structure of Materials*, vol. 1. Litera, Kiev (in Russian).
- Guz, A. N.** (2008b): *Fundamentals of The Compressive Fracture Mechanics of Composites: Related Mechanics of Fracture*, vol. 2. Litera, Kiev (in Russian).
- Guz, A. N., Nazarenko, V. M.** (1985a): Theory of near-surface delamination of composite materials under compression along the macro-crack. *Mech. Comp. Mater.*, vol. 21(5), pp. 826-833.
- Guz, A. N., Nazarenko, V. M.** (1985b): Symmetric failure of the half-space with penny-shaped crack in compression. *Theor. Appl. Fract. Mech.*, vol. 3, pp. 233-245.
- Hoff, N. J.** (1954): Buckling and stability. *J. Roy. Aeron. Soc.* 58(1).
- Hutchinson, J.W., He, M.Y., Evans, A.G.** (2000): The influence of imperfections on the nucleation and propagation of buckling driven delaminations. *J. Mech. Phys. Solids*, vol. 48, pp. 709-734.
- Hutchinson, J.W., Suo, Z.** (1992): Mixed mode cracking in layered materials. *Adv. Appl. Mech.*, vol. 29, pp. 63-191.
- Hutchinson, J.W., Thouless, M.D. and Liniger, E. G.** (1992): Growth and configurational stability of circular, buckling-driven film delaminations. *Acta Metall. Mater.*, vol. 40, pp. 295-308.
- Hwang, S.F., Mao, C.P.** (1999): The delamination buckling of single-fibre system and interply hybrid composites. *Compos. Struct*, vol. 46, pp. 279-287.
- Kachanov, L. M.** (1976): Fracture of composite materials by means a delamination. *Mechanika Polimerov*, vol. 5, pp. 918-922.
- Kardomateas, G. A., Pelgri, A. A., Malik, B.** (1995): Growth of internal delaminations under cyclic compression in composite plates. *J. Mech. Phys. Solids*, vol. 43(6), pp. 847-868.
- Moon, M.W., Chung, J.W., Lee, K.R., Oh, K.H., Wang, R., Evans, A.G.** (2002): An experimental study of the influence of imperfections on the buckling of compressed thin films. *Acta Materialia*, vol. 50, pp. 1219-1227.
- Moon, M.W., Lee, K.R., Oh, K.H., Hutchinson, J.W.** (2004): Buckle delamination on patterned substrates. *Acta Materialia*, vol. 52, pp. 3151-3159.
- Nilsson, K. F., Giannakopoulos, A.E.** (1995): A finite element analysis of con-

figurational stability and finite growth of buckling driven delamination. *J. Mech. Phys. Solids*, vol. 43, pp. 1983-2021.

Nilsson, K. F., Thesken, J.C., Sindelar, P., Giannakopoulos, A.E., Stoakers, B. (1993): A theoretical and experimental investigation of buckling induced delamination growth. *J. Mech. Phys. Solids*, vol. 41, pp. 749-782.

Rabotnov, Yu N. (1977): *Elements of Hereditary Mechanics of Solid Bodies*, Nauka, Moscow (in Russian).

Rzayev O. G., Akbarov S. D. (2002): Local buckling of the elastic and viscoelastic coating around the penny-shaped interface crack. *Int. J. Eng. Sci.*, vol. 40, pp. 1435-1451.

Rzayev O. G. (2002): Local buckling around an interfacial crack in a viscoelastic sandwich plate. *Mechanics of Composite Materials*, vol. 38 (2), pp. 233-242.

Schapery, R.A. (1966): Approximate methods of transform inversion for viscoelastic stress analyses. *Proc. US Nat. Cong. Appl. ASME*, pp. 1075-1085.

Short, G.J., Guild, F.J., Pavier, M.J. (2001): The effect of delamination geometry on the compressive failure of composite laminates. *Compos. Sci. Technol.*, vol. 61, pp. 2075-2086.

Thouless, M. D., Jensen, H.M., Liniger, E.G. (1994): Delamination from edge flaws. *Proc. Royal Soc. London A447*, 271-279.

Volmir, A.S. (1967): *Stability of Deformation Systems*, Nauko, Moscow.

Wang, J. T., Cheng, S. H., Lin, C. C. (1995): Local buckling of delaminated beams and plates using continuous analysis. *J. Compos. Mater.*, vol. 29, pp. 1374-1402.

Wang, J.-S., Evans, A.G. (1998): Measurement and analysis of buckling and buckle propagation in compressed oxide layers on super ally substrates. *Acta Mater.*, vol. 46, pp. 4993-5505.

